# Channel estimation in mobile wireless systems

IDD PAZI ALLI


KTH Electrical Engineering

Master's Degree Project
Stockholm, Sweden

XR-EE-SB 2012:005

# Channel estimation in mobile wireless systems

Signal Processing Lab

School of Electrical Engineering (EES)

Royal Institute of Technology

Stockholm

By

Idd Pazi Alli

Supervisor & Examiner

Dr. Joakim Jaldén

# TABLE OF CONTENTS

# LIST OF FIGURES

## LIST OF TABLES

## LIST OF ABBREVIATIONS AND ACRONYMS

| | |
|---|---|
| 3G | 3rd generation (Mobile telephony) |
| 3GPP | 3rd generation partnership project |
| 3GPP2 | 3rd generation partnership project 2 |
| 4G | 4th generation |
| AWGN | Additive White Gaussian Noise |
| B3G | Beyond 3rd generation |
| BS | Base Station |
| BEM | Basis Expansion Model |
| CDL | Clustered Delay Line |
| CDMA | Code Division Multiple Access |
| CIR | Channel Impulse Response |
| DS | Delay Spread |
| DFT | Discrete Fourier Transform |
| DS spread spectrum | Direct Sequence Spread Spectrum |
| DPSS | Discrete Prolate Spheroidal Sequences |
| DTFT | Discrete Time Fourier Transform |
| DVB | Digital Video Broadcasting |
| E TRA | Evolved Universal Terrestrial Radio Access |
| E TRAN | Evolved Universal Terrestrial Radio Access Network |
| FDM | Frequency Division Multiplexing |
| FFT | Fast Fourier Transform |
| GSCM | Geometry-based Stochastic Channel Models |
| ICI | Inter-Channel Interference |
| IFFT | Inverse Fast Fourier Transform |
| ISI | Inter-symbol interference |
| ITU-R | International Telecommunication Union Radiocommunication Sector |
| KTH | Royal Institute of Technology Stockholm |
| LOS | Line of sight |
| LMSE | Least Mean Square Error |
| LS | Large Scale |
| LTE | Long Term Evolution |
| MA | Moving Average |
| MC-CDMA | Multi-Carrier Code Division Multiple Access |
| MC-DS-CDMA | Multi-Carrier Direct Sequence Code Division Multiple Access |
| MIMO | Multiple Input Multiple Output |

| | |
|---|---|
| MS | Mobile Station |
| MMSE | Minimum Mean Square Error |
| MSE | Mean square error |
| NLOS | Non Line of sight |
| OFDM | Orthogonal Frequency Division Multiplexing |
| PN | Pseudo-random Noise |
| RMS | Root Mean Square |
| SCM | Spatial Channel Model |
| SFN | Single Frequency Networks |
| TU | Typical Urban |
| UE | User Equipment |
| UMTS | Universal Mobile Telecommunications System |
| WINNER | Wireless World Initiative New Radio |
| WLAN | Wireless Local Area Network |
| WMAN | Wireless Metro Area Network |
| WSSUS | Wide Sense Stationary Uncorrelated Scattering |

## Nomenclature

References are indicated by bracket [] and can consist a reference to a particular page. The number in the bracket refers to the reference which can be found at the back of the main report on page 45. Reference to equations are indicated by "(a.b.c)" where a is a section number, b and c are counting variable of the corresponding element in the section. A vector denoted by boldface lowercase letter "**x**" and matrix by boldface uppercase letter "**X**".

**Acknowledgement**

I would like to thank the Signal Processing Lab at the Royal Institute of Technology (KTH) for allowing me to do my Master thesis. Special gratitude goes to my supervisor and examiner Dr. Joakim Jaldén who assisted me with ideas, methods, moral support, and guidance throughout the time of doing my thesis which would have been impossible without his help. I would also like to give my thanks to Dr. Mats Bengtsson for his help during my thesis.

## Abstract

The demands of multimedia services from mobile user equipment (UE) for achieving high data rate, high capacity and reliable communication in modern mobile wireless systems are continually ever-growing. As a consequence, several technologies, such as the Universal Mobile Telecommunications System (UMTS) and the 3rd Generation Partnership Project (3GPP), have been used to meet these challenges. However, due to the channel fading and the Doppler shifts caused by user mobility, a common problem in wireless systems, additional technologies are needed to combat multipath propagation fading and Doppler shifts. Time-variant channel estimation is one such crucial technique used to improve the performance of the modern wireless systems with Doppler spread and multipath spread.

One of vital parts of the mobile wireless channel is channel estimation, which is a method used to significantly improve the performance of the system, especially for 4G and Long Term Evolution (LTE) systems. Channel estimation is done by estimating the time-varying channel frequency response for the OFDM symbols. Time-variant channel estimation using Discrete Prolate Spheroidal Sequences (DPSS) technique is a useful channel estimation technique in mobile wireless communication for accurately estimating transmitted information. The main advantage of DPSS or Slepian basis expansion is allowing more accurate representation of high mobility mobile wireless channels with low complexity. Systems such as the fourth generation cellular wireless standards (4G), which was recently introduced in Sweden and other countries together with the Long Term Evolution, can use channel estimation techniques for providing the high data rate in modern mobile wireless communication systems.

The main goal of this thesis is to test the recently proposed method, time-variant channel estimation using Discrete Prolate Spheroidal Sequences (DPSS) to model the WINNER phase II channel model. The time-variant sub-carrier coefficients are expanded in terms of orthogonal DPS sequences, referred to as Slepian basis expansions. Both Slepian basis expansions and DPS sequences span the low-dimensional subspace of time-limited and band-limited sequences as Slepian showed. Testing is done by using just two system parameters, the maximum Doppler frequency $v_{D\max}$ and K, the number of basis functions of length $N$ = 256.

The main focus of this thesis is to investigate the Power spectrum and channel gain caused by Doppler spread of the WINNER II channel model together with linear fitting of curves for both the Slepian and Fourier basis expansion models. In addition, it investigates the Mean Square Error (MSE) using the Least Squares (LS) method. The investigation was carried out

by simulation in Matlab, which shows that the spectrum of the maximum velocity of the user in mobile wireless channel is upper bounded by the maximum normalized one-sided Doppler frequency. Matlab simulations support the values of the results. The value of maximum Doppler bandwidth $\nu_{D\max}$ of the WINNER model is exactly the same value as DPS sequences. In addition to the Power spectrum of the WINNER model, the fitting of Slepian basis expansion performs better in the WINNER model than that of the Fourier basis expansion.

**Keywords:** Time-variant channel, Discrete Prolate Spheroidal Sequences (DPSS), Slepian Basis Expansion, WINNER (Wireless World Initiative New Radio) phase II model, Basis functions K.

# 1. INTRODUCTION

Channel estimation is an important technique especially in mobile wireless network systems where the wireless channel changes over time, usually caused by transmitter and/or receiver being in motion at vehicular speed. Mobile wireless communication is adversely affected by the multipath interference resulting from reflections from surroundings, such as hills, buildings and other obstacles. In order to provide reliability and high data rates at the receiver, the system needs an accurate estimate of the time-varying channel. Furthermore, mobile wireless systems are one of the main technologies which used to provide services such as data communication, voice, and video with quality of service (QoS) for both mobile users and nomadic. The knowledge of the impulse response of mobile wireless propagation channels in the estimator is an aid in acquiring important information for testing, designing or planning wireless communication systems.

Channel estimation is based on the training sequence of bits and which is unique for a certain transmitter and which is repeated in every transmitted burst [35]. The channel estimator gives the knowledge on the channel impulse response (CIR) to the detector and it estimates separately the CIR for each burst by exploiting transmitted bits and corresponding received bits. Signal detectors must have knowledge concerning the channel impulse response (CIR) of the radio link with known transmitted sequences, which can be done by a separate channel estimator. The modulated corrupted signal from the channel has to be undergoing the channel estimation using LMS, MLSE, MMSE, RMS etc before the demodulation takes place at the receiver side. The channel estimator is shown in figure 1.1.

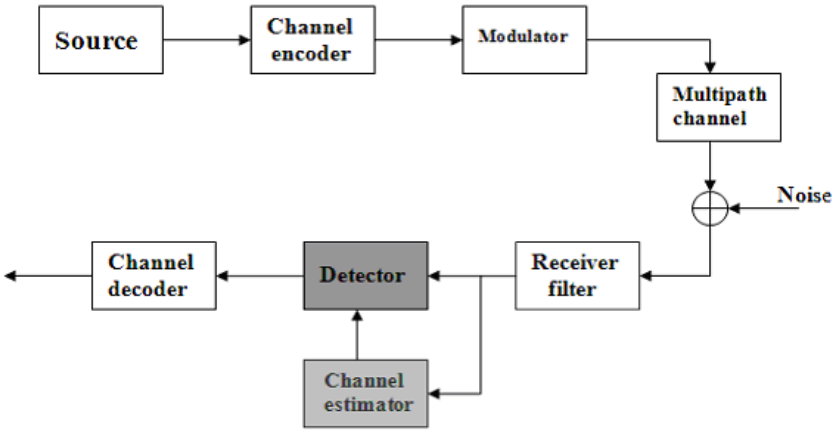


Figure 1.1 The block diagram of the channel estimator

Advanced technologies are needed to be developed in order to increase the capacity, high data rate, lower latency, and packet-optimized system that supports multiple Radio Access Technologies (RATs). The current generation of mobile telecommunication networks called the pre-4G standard, is a step towards the advanced LTE, which is an enhancement to Universal Mobile Telecommunication Systems (UMTS). LTE is a variant of the next generation of mobile telephone.

The main feature of the next generation of mobile wireless communication system is to deliver high data rate. 3GPP Long Term Evolution is a project name within the third Generation Partnership Project (3GPP) Release 8 [37].

The LTE project is not a standard, but it will help to modify the new UMTS mobile standard for the future requirement. LTE is identified as the universal terrestrial radio access (E UTRA) and as the universal terrestrial radio access network (E UTRAN) which is based on conventional OFDM as shown in [29]. The key aim of the LTE will be as good as the 3GPP High Speed Packet Access (HSPA) technology. The worldwide carriers including the ones in the United States, has announced plans to convert their current networks to LTE beginning 2009. In 2009 the European Commission also had a plan to invest about 18 million Euro in LTE deployment research and putting forward, a future 4G system [31].

The use of DPSS together with the Fourier basis expansion is to be tested in order to model the WINNER phase II channel model. The WINNER phase II model is to be compared with the other two time-varying channel estimation methods; the Slepian basis expansion and Fourier basis expansion using basis functions K. The basis functions are to be used in order to determine the Mean Square Error (MSE) by using the Least Squares (LS) method.

## 1.1 The fourth generation standards (4G) and 3GPP LTE

The fourth generation of the cellular wireless standards (4G) is developed to increase the capacity and speed of the mobile telephones networks and it is the next step toward LTE advanced. 4G is considered an all-IP packet-switched network. It has at least 200kbits/s, is a multi-carrier transmission and is the successor to 3G. Users of 4G have access to ultra-broadband internet, IP telephony, gaming services and streamed multimedia. In high mobility the data rate of 4G can reach up to 100 Mbit/s in the downlink and 50 Mbit/s in the uplink. In contrast 4G can reach 1.0 Gbit/s in low mobility as nomadic/local wireless access. The 4G standard can provide the services up to 40 MHz wide channels. The fourth generation is frequency-domain equalization schemes based on OFDM technique together with MIMO technology. 4G is used mostly in multi-carrier transmission [32]. The aim for the LTE is to have the download speed up to 100 Mbit/s and mobility is supported for up 350 km/h [8].

## 1.2 Doppler effect

The name Doppler comes from the Austrian physicist Christian Doppler who described the Doppler effect in 1842 in Prague. Doppler shift $D_i$ is the change in frequency of the wave when an observer, source or medium are in motion i.e. the user moves with velocity $v$. Doppler shift relates to multipath component delays and angle of arrival of the propagation components of the waves as shown in figure 1.2.

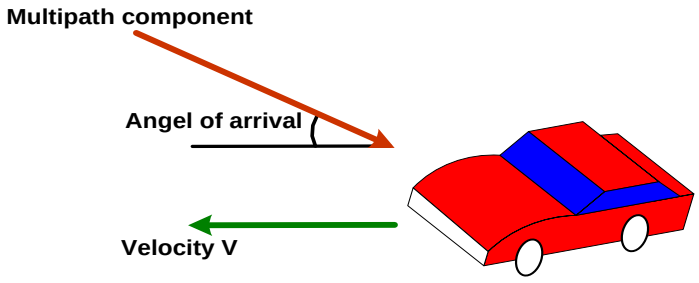


Figure 1.2 Doppler shift of i-th multipath component of the scatted waves

The Doppler shift for a multipath component is given as:

$$D_i = \frac{v_{\max}}{\lambda} \cos \alpha_i \tag{1.1}$$

Where:

$v_{\max}$ : Maximum velocity of the mobile user

$\alpha_i$ : Angle of arrival of the signal relative to the direction of the user

From equation (1.1) we rewrite the Doppler shift of the i-th component of the wave as:

$$D_i = f_{D\max} \cos \alpha_i \tag{1.2}$$

Where:

$f_{D\max}$ : Maximum Doppler frequency

and

$$f_{D\max} = \frac{v_{\max}}{c_0} f_C \tag{1.3}$$

Where:

$f_C$ : Carrier frequency

$c_0$ : Speed of light

## 1.3 Discrete Prolate Spheroidal Sequences (DPSS)

It has shown in [2] that the DPSS is very suitable for estimating the time-variant channel and this explains why using the DPS sequences in time-variant channel estimation is very suitable for the fourth generation of cellular wireless standards (4G) and for the Long Term Evolution (LTE) models. We need to model accurately the time-variant channel because of the present of Doppler shift in the mobile wireless systems. In [2] it was also shown that the Slepian basis expansion is suitable for the modeling of a time-variant frequency-selective channel for the duration of a data block.

This thesis tests these Discrete Prolate Spheroidal Sequences and these DPS sequences are common among several methods used in time-variant channel estimation. Discrete Prolate Spheroidal Sequences are defined as the solutions to a matrix eigenvalue problem [23, 40]. DPSS describe the subspace of band-limited sequences. The model was proposed just a few years ago and still considered new. The DPSS has the advantage of having a double orthogonal property over both finite as well as infinity sets and the model can be used to any sets of orthogonal basis functions [10].

Discrete Prolate Spheroidal Sequences can be used to estimate a downlink of the time-variant frequency-selective channels for a mobile wireless communication system. The channel estimator is using a multiuser multicarrier code division multiple access (MC-CDMA) based on orthogonal frequency division multiplexing (OFDM) as explain in [2]. Thomas Zemen and Christoph Mecklenbräuker are the first one to estimate mobile wireless channel using the

Slepian sequences and they came to conclude that the maximum normalized variation of wireless channels in frequency domain is upper bounded by the maximum normalized one-sided Doppler frequency [2]. The maximum Doppler bandwidth caused by Doppler spread can be described as:

$$v_{D\max} = \frac{v_{\max} f_C}{c_0} T_S \tag{1.4}$$

$v_{D\max}$ : Normalized maximum Doppler bandwidth

$v_{\max}$ : Maximum velocity of the user (vehicular speed)

$f_C$ : Carrier frequency

$T_S$ : Symbol time with symbol rate $R_s = 1/T_s$

$c_0$ : The speed of light

## 1.4 WINNER phase II channel model

The Winner II channel model is modeled by the use of DPS sequences in this thesis was developed by and applied within the European Wireless World Initiative New Radio project (WINNER). The WINNER model has been developed widely accepted and suitable propagation parameters of a Beyond-3G (B3G) wireless communication systems at the link level and at a system level. Winner model describes the suitable radio channel models especially with IEEE 802.16m and ITU-R/8F standards.

The Royal Institute of Technology (KTH) together with other partners within WINNER Work Package 1 (WP1) [See Appendix A.1] have involved and created the new radio channel estimation model based on existing 3GPP/3GPP2 Spatial Channel Model (SCM) which is used in outdoor environment and IEEE 802n in indoor for estimating the radio channels as explained in [28]. The WINNER model project uses a channel bandwidth of up to 100 MHz for a one radio link and between 2 and 6 GHz for the radio frequencies [1]. The model can be applied not only to WINNER II system, but also any other wireless system operating in the frequency range between 2 and 6 GHz. WINNER II system supports multi-user, MIMO technology, polarization, multi-cell, and multi-hop networks.

## 1.5 3GPP/3GPP2 Spatial Channel Model (SCM)

The third Generation Partnership project is based on CDMA2000, which is a standard for 3G. The spatial channel used in the WINNER model is based on multiple-input multiple-output (MIMO) technology, i.e. multiple transmitters and multiple receivers. The WINNER model is based on Geometry-based stochastic channel models (GSCM), which enables both testing and simulation of mobile communication systems. There are several different random parameters used in the WINNER II channel model: a delay spread, delay values, shadow fading, angle spread, and path loss. The Spatial Channel Modeling (SCM) is a CDMA system, and a geometric or rays-based model in B3G standard designed especially for frequencies range between 5 and 100 MHz and a center frequency of 2 GHz [22]. The Spatial Channel Model is developed from 3GPP and the model is used in the cellular networks especially for three environments suburban macro-cells, urban macro-cells and urban micro-cells. The main aim of the SCM model is to model the radio channels. 3GPP Spatial Channel Model Extended (SCME) which used in the WINNER II channel model is an extension to 3GPP Spatial

Channel Model (SCM).

## 1.6 Orthogonal Frequency Division Multiplexing (OFDM)

The channel estimation methods based on OFDM are discussed in [2, 10, 11].
Orthogonal frequency division multiplexing can accommodate high data rate in the mobile wireless systems in order to handle multimedia services. It is important to understand the OFDM technology because the channel estimation is an integral part of OFDM system. OFDM technology can be used effectively to avoid the effect of frequency-selective fading and narrowband interference from parallel closely spaced frequencies in mobile networks. If there is no orthogonality in the channel, inter-channel interference (ICI) can be experienced. With these vital advantages, OFDM technology has been widely used by many wireless standards such as WLAN, WMAN, and DVB [38]. In OFDM scheme, complex filters are not required and time-spreading can be used without any complications in OFDM scheme.

OFDM scheme can also help to manage the single frequency networks (SFN) by sending the same signals at the same frequency using adjacent transmitters without interfering each other. OFDM has been popularly used for various wireless communication systems such as fourth generation 4G wireless system. Since we want to test and evaluate the use of Digital Prolate Spheroidal Sequences based on OFDM technology, we give a brief introduction to OFDM system. Orthogonal frequency-division multiplexing (OFDM) is based on the frequency-division multiplexing (FDM) scheme used as digital multi-carrier modulation method, particularly in estimating a channel in two-dimensions (time – frequency lattice) [41]. The technology is intended for downlink in the physical layer. The OFDM channel is divided into several narrowband sub-carriers and designed to be orthogonal with each other in the frequency domain for carrying data symbols. Each sub-carrier has parallel narrow band-pass channels at low symbol rate. The advantage of using a low symbol rate is that it is possible to use a guard interval between symbols and to avoid the inter-symbol interference. In the OFDM the total data rate for sub-carriers are equivalent to the single carrier modulation with the same bandwidth. The OFDM plays an important role in the wideband of mobile wireless systems [20].

### 1.6.1 Advantages of OFDM

The OFDM methods can help the mobile wireless channel transmit large amounts of data through the mobile channel. The carrier of the OFDM has a low bit rate data stream, which enables the system to have high data rate, high data capacity, as well as eliminating the inter-symbol interference (ISI) in the system. The OFDM technology uses the efficient Fast Fourier Transform algorithm which reduces complexity of modulation/demodulation process. OFDM is less sensitivity to the error caused by time synchronization of the network. OFDM technology works well because it can avoid and eliminate the inter-symbol interference (ISI) as well as the fading caused by multipath propagation [7, 9].

### 1.6.2 The disadvantage of the OFDM

The technology is very sensitive to the Doppler shift that is very common in mobile wireless communication systems. OFDM is very sensitive to frequency synchronization errors. Moreover, the overall efficiency reduces by inserting cyclic prefix /guard interval [21].

### 1.6.3 Multi-Carrier Code Division Multiple Access (MC-CDMA)

Another interesting scheme based on OFDM is called Multi-carrier code division multiple access (MC-CDMA). This scheme is also used when DPSS has been analyzed in [2]. These (MC-CDMA) types of schemes are used in scenarios where a large number of arbitrary located users want quick access to the mobile wireless channel as well as when users share the radio spectrum [33, 34]. Both OFDM and CDMA schemes are well-suited for providing frequency diversity, which improves the performance of data transmission over fading mobile wireless channel.

MC-CDMA is considered as direct-sequence CDMA signal which is processed by the Inverse Fast Fourier Transform (IFFT) before it has transmitted. MC-DS-CDMA where OFDM is regarded as the modulation scheme, the data symbols of each subscriber are spread in time by multiplying the chips on a pseudo-random noise (PN) code by data symbol on the sub-carrier [30]. The disadvantage of DS-CDMA is that the signals are not orthogonal, and it can cause interference among users. A good reason for using MC-CDMA scheme is its ability to reconstruct the signal received from other sub-carriers after the mobile wireless communication has been influenced by frequency-selective channels [7].

## 1.7 Outline of the thesis

The main reason for using time-variant channel estimation of modern mobile wireless communication systems is to achieve a reliable mobile wireless system by increasing the capacity, bandwidth efficiency, and the data rate.

This thesis is divided into eight sections

- Section 2 introduces of time-variant wireless communication channel.
- Section 2.1 describes the channel fading of the multipath propagation.
- In Section 2.2 the signal propagation model and parameters are presented.
- Section 2.3 highlights the previous related works.
- Section 3 gives the description of the problem statement of the thesis.
- Section 4 describes the system model and signal model for WINNER, Slepian and Fourier basis expansion.
- Section 4.1 describes the basic expansion, Discrete Prolate Spheroidal Sequences (DPSS).
- Section 4.2 explains the signal model for flat fading time-variant channel for the Discrete Prolate Spheroidal Sequences.
- Section 4.3 describes the time- variant frequency-selective channel estimation

- Section 4.4 explains the signal model for Fourier basis expansion which is one of the basis expansion methods (BEM) used in this thesis.
- Section 4.5 and 4.6 describe the WINNER phase II channel model which has been used to generate the radio channel realizations for link level simulation in this thesis.
- In section 5 we explain the power spectrum estimation of the time-variant channel effected by the Doppler shifts produced by user mobility.
- Section 5.1 and 5.2 explain the periodogram, the method which used to estimate the power spectrum of the WINNER model.
- In section 6 we demonstrate simulation results and analysis.
- In section 7 the analytical and numerical results have been discussed.
- The last section 8 concludes the thesis, and gives suggestions for future work.

## 2. Time-variant channel

A time-variant channel is a channel which has the property of changing over time. The time-variant channel has the characteristic of a signal which changes at the same rate as the changes in the communication signal, or even faster. The channel normally has the Doppler effect which caused by Doppler spread of multipath propagation. A time-invariant channel can be modeled as a linear filter with impulse response $h(t)$ and its Fourier transform, the system function $H(f)$. Let $h(t)$ be the transmitted sequence over a time-invariant channel $h(t)$, then the received sequence $y(t)$ is given in the time domain by:

$$y(t) = h(t) * x(t) + n(t) \tag{2.1}$$

Where:

$n(t)$ : Additive White Gaussian Noise (AWGN) with zero mean and variance $E\{|n(t)|\} = \sigma_n^2$

$*$ : Denote the convolution

The time-variant system is the system which is effected by either relative motion between user who is moving with the velocity $v$ or by movement of objects in the channel. This channel has either the same changing or one that is faster than the rate of the communication signal. The model for mobile wireless channel with additive white noise in time domain can be written as:

$$y(t) = \sum_{i}^{N} \alpha_i(t) x(t - \tau_i(t)) + n(t) \tag{2.2}$$

Where:

$\alpha_i(t)$ : The i-th component time-variant amplitude at time instant $t$

$x(t-\tau_i(t))$ : Transmitted symbol at time $t-\tau_i(t)$

$\tau_i(t)$ : The i-th component propagation delay at time $t$

$n(t)$ : Additive White Gaussian Noise (AWGN) with zero mean and variance $E\{|n(t)|\} = \sigma_n^2$

The linear time-variant channel from the multipath propagation of the frequency selective channel is a filter with the following baseband equivalent impulse response [14]:

$$h(\tau,t) = \sum_{i=1}^{N} \alpha_i(t) e^{j\theta_i(t)} \delta(t-\tau_i) \tag{2.3}$$

Where:

$h(\tau,t)$ : Impulse response of a channel at instant time $\tau$

$\alpha_i$ : The i-th component time-variant complex amplitude

$\theta_i$ : The i-th component phase

$\tau_i$ : The i-th delay

$\delta(\cdot)$ : Kronecker delta function

$N$ : Number of resolvable multipath components

$e^{j\theta_i(t)}$ : Phase rotation with carrier frequency $f_C$ and delay $\tau_i(t)$

The channel impulse response $h(\tau,t)$ represents a Doppler spectrum and has a band-limited in $[-v_{D\max}, v_{D\max}]$ according to [2].

If we want to express the complex-valued, baseband time-variant impulse response in terms of the effect of the transmit filter $h_T(\tau)$ together with the matched receive filter $h_R(\tau)$, the time-variant channel model can be expressed as [12]:

$$h'(\tau,t) = h_T(\tau) * h(\tau,t) * h_R(\tau) \tag{2.4}$$

Where:

$h_T(\tau)$ : Transmit filter

$h_R(\tau)$ : Matched receive filter

$*$ : Denotes convolution

The Fourier transformer of the frequency response can be written as:

$$H(t;f) = \int_{-\infty}^{\infty} h(\tau,t) e^{-j2\pi\tau} d\tau \tag{2.5}$$

Figure 2.1 shows the different delay taps at the receiver side and the only one signal which transmitted at the transmitter.

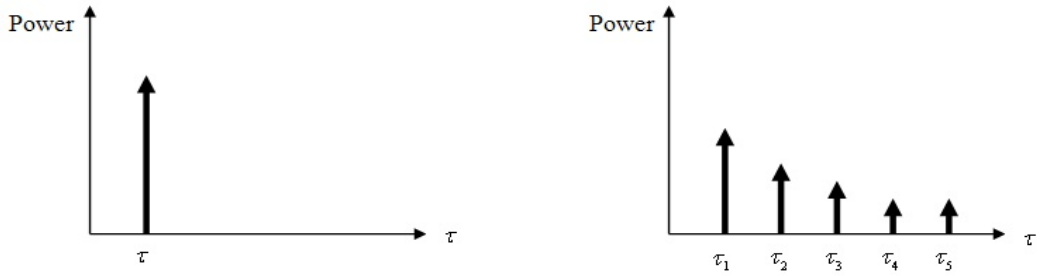


a) Transmitter b) Receiver

Figure 2.1 Power delay profile of the multipath channel with delay $\tau_i$

The channel estimation of the time-variant frequency response $h_i[m]$ can significantly improve the performance of the receiver. The discrete time baseband at the receiver signal from Equation (2.2) in terms of channel filter taps can be written as [3]:

$$y[m] = \sum_{i}^{N} h_i[m]\, x[m-i] + n[m] \tag{2.6}$$

Where:

$n[m]$ : Down-converted low pass filtered noise

## 2.1 Channel fading

The multipath propagation and the shadowing caused by isolated obstacles, such as mountains, buildings, trees etc., between the transmitter and the receiver. The signal fading is created by user mobility through these isolated obstacles. A signal transmitted over mobile wireless fading channel is deteriorated due to several causes. In time-variant channel, it is the Doppler spread which gives information about the fading rate of the channel, while in the other hand the channel fading causes a loss in signal power at the same time increases a power of noise. The error caused by multipath propagation in mobile communication channel can cause inter-symbol interference (ISI) at the receiver side. A channel affected by fading has to be compensated by channel equalization based on the channel estimates before reliable detection of the transmitted information bits can be done.

The individual reflected waves which influence the signal propagation can be modeled as Wide Sense Stationary Uncorrelated Scattering (WSSUS). A time-varying frequency-selective wireless channel is usually modeled as WSSUS process [39]. The WSSUS means that one received delay $\tau_i$ component of the signal is uncorrelated with other multipath component delays. In this thesis we have assumed that the time-variant multipath channel $h(\tau,t)$ is fading and the channel is modeled as the Wide Sense Stationary Uncorrelated Scattering and has Doppler power spectrum modeled in Jakes [36].

$$R(\tau) = J_0(2\pi D\tau) \tag{2.7}$$

Where

$D$ : Maximum Doppler shift

For the Stochastic Channel Models, we can take the Fourier transform of an impulse response $h(\tau,t)$ and we get $H(f,t)$ which is the system function of the channel. According to our assumption about wide sense stationarity in time $t$, we may compute the autocorrelation function $\phi_H(f_1, f_2; \Delta t)$ of the time-variant multipath channel as [6]:

$$\phi_H(f_1, f_2; \Delta t) = E\{H(f_2; t+\Delta t) H^*(f_1; t)\} \tag{2.8}$$

For WSSUS channels, we can rewrite Equation (2.8) as:

$$\phi_H(f_1, f_2; \Delta t) = \int_{-\infty}^{\infty} \phi_H(\tau; \Delta t) e^{-j2\pi\tau(f_2 - f_1)} d\tau = \phi_H(\Delta f; \Delta t) \tag{2.9}$$

Where

$\phi_H(\Delta f; \Delta t)$ : Frequency-time correlation function
$\Delta f = f_2 - f_1$ : Frequency difference
$\Delta t$ : Time difference between channel system function

By setting $\Delta t = 0$ in Equation (2.9) we can get:

$$\phi_H(\Delta f; 0) = \phi_H(\Delta f) \tag{2.10}$$

Where:

$\phi_H(\Delta f)$ : Fourier transform of the intensity profile function $\phi_H(\tau)$.

Shadow fading which is a medium-scale propagation component occurs when the isolated obstacles stays between the receiver and the signal transmitter. The shadow fading which created from obstacles causes a significant reduction in signal power due to the shadowed or blocked signal by obstacles. Shadow fading normally lasts several seconds or minutes but the multipath fading has much faster time-scale.

When the delay constraint of the channel is less than the coherence time, we have slow fading but when the delay constraint of the channel is larger, the channel is undergoes fast fading which is a temporary deep fading. A slow fading channel usually has deep fading which makes difficult to recover the transmitting information from the sender. By investigating the scattering factor or channel spread factor, as it sometimes called, helps to understand the characteristic of the channel whether a channel of the wireless channel is slow or fast. If the scattering factor is less than one, the channel is said to be a slowly flat fading, and if the scattering factor is larger than one, we say the channel is overspread. The channel spread factor is the product of the $T_d B_d$ (see Section 2.2). The scattering factor of a mobile wireless is normally underspread and the scattering factor is given by:

$$T_d B_d \approx \frac{1}{B_C T_C} << \frac{1}{W T_S} \approx 1 \tag{2.11}$$

Where:

$W$ : The signal bandwidth
$T$ : The symbol duration
$T_C$ : Coherence time
$B_C$ : Coherence bandwidth
$T_d$ : Delay spread
$B_d$ : Doppler spread

### 2.1.1 Rayleigh fading distribution

Rayleigh fading is a model that models the scatted signal of a wave between the transmitter and receiver, i.e. none of signal paths is dominant and each multipath of the signal will vary and can have an impact on the overall signal at the receiver. It is a kind of fading that is often experienced a large number of reflection points which created in a well built up urban environment.

Rayleigh fading model is reasonable model to model a heavily built-up city centers like Manhattan in New York. The model is considered as the flat fading of the component $i$ of the multipath channel filter taps $h_i[m]$, provided that the tap gains are circularly complex Gaussian random variables with zero mean. The Rayleigh distribution is normally modeled for Non line of sight (NLOS). The Rayleigh distribution is given by:

$$f(x) = \frac{x}{\sigma^2} e^{\frac{-x^2}{2\sigma^2}} \qquad x \geq 0 \tag{2.12}$$

Where:

$\sigma^2$ : Time-average power of the received signal before envelope detection

For the Line of sight (LOS) where one component is stronger than other components, we have a distribution which is called Nakagami-Rice or sometimes known as Rician distribution with nonzero mean. The channel filter taps of Rician distribution is given as follows:

$$f(x) = I_0\left(\frac{x\alpha}{\sigma^2}\right)\frac{x}{\sigma^2} e^{\frac{-x^2+\alpha^2}{2\sigma^2}} \qquad x \geq 0 \tag{2.13}$$

Where:

$I_0$ : Modified Bassel function of the first kind with order zero
$\alpha$ : Amplitude of the strong component (LOS) of constant signal

When $\alpha$ is zero the Rician distribution will be reduced to Rayleigh distribution.

The receiver receives the scattered signal from the transmitter and these scattered signals cause the Doppler spread and the fading. Figure 2.1.1 shows different obstacles between the transmitter and the receiver and five different components of multipath propagation produced

by isolated obstacles. In general, the receiver receives the electromagnetic waves of different paths from the Base Station (BS) in the mobile wireless channels.

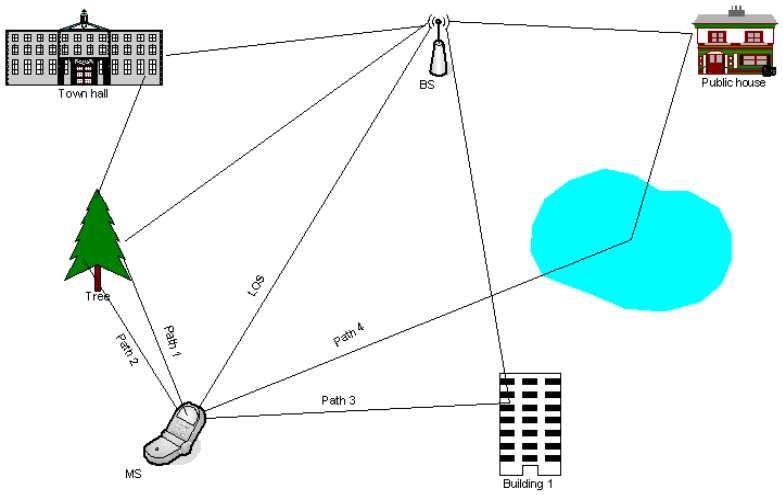


Figure 2.1.1 Multipath propagation phenomena of the signal from the transmitter (BS) to the receiver (MS)

Figure 2.1.2 shows the network layout of the WINNER model with the segments of the car moving at different distances shown in green color. In the figure shows also multiple links. The simulation of the WINNER model in this thesis is done with only one radio link with small-scale parameters as it can be seen in the figure marked with blue dashed lines.

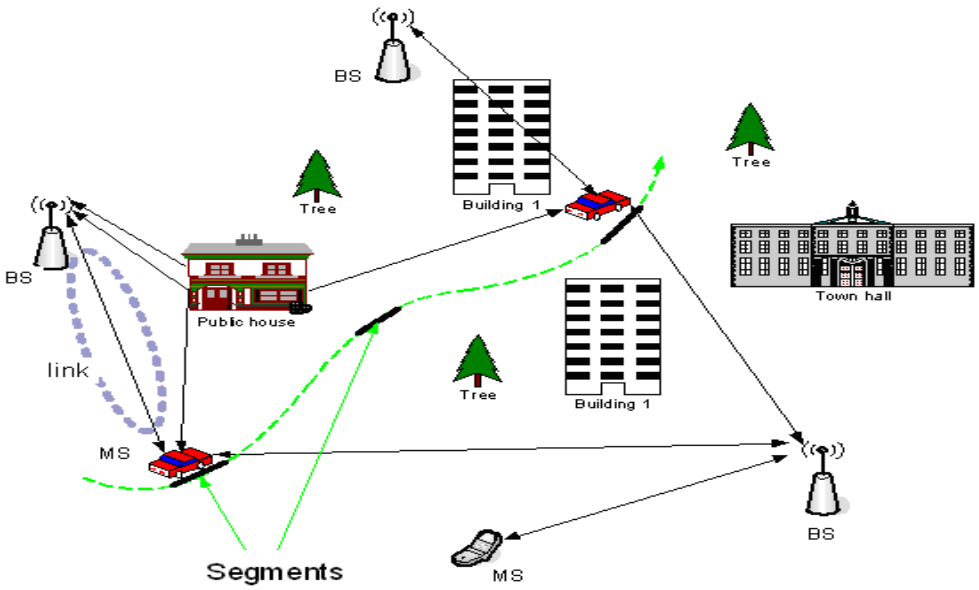


Figure 2.1.2 The Network layout for one radio link for WINNER model

## 2.2 Channel propagation and parameters

Most mobile wireless communication channels are multipath and time-varying channels. The reflected waves arrive at the receiver with different path delays, fluctuations in signal's amplitude, angle of arrival and change in phase. Wireless mobile channels normally are effected by Doppler shift caused by user mobility, and the reflected waves have Doppler

spread which is caused mainly by multipath propagation [18]. The narrow-band channel of the Doppler spread is usually equivalent to maximum delay shift.

The following sections discuss the important parameters of a mobile wireless channel.

### 2.2.1 Doppler spread

Doppler spread and coherence time are parameters which explain the time-varying of the channel in a small-scale region. Doppler spread is a measure of spectral broadening caused by the time rate of change of the mobile wireless channel or it may be explained as a measure of how fast the taps $h_i[m]$ vary with time index $m$. In another words, the largest deferent between the multipath components in Doppler shift causing to a single fading channel tap is define as the Doppler spread.

The Doppler spread is also defined as the power spectrum of the nonzero frequency range, and it relates to the multipath component delays as well as angle of arrival of the scatted waves. Doppler spread is normally on the order of 10 milliseconds. Doppler spread can be expressed as [3]:

$$B_s = \max_{i,j} f_c \left| \tau_i(t) - \tau_j(t) \right| \tag{2.14}$$

Where:

$f_C$ : Carrier frequency

When the user moves with a high speed, the Doppler spread will be large but at the same time the coherence time will be small. This is because Doppler spread is the reciprocal of the coherence time of the channel.

### 2.2.2 Coherence time

The time over which taps $h_i[m]$ change rapidly as a function of time $m$ is called the coherence time $T_C$. It is necessary in mobile wireless channels to determine the time coherence in order to know the Doppler spread of the channel. Both Doppler spread and coherence time are parameters which describe the time-variant of the multipath channel in small-scale region. The smaller the time coherence, the larger the Doppler spread. If the symbol time $T_S$ is less than coherence time $T_C$, there is no change in the channel (correlated channel). The coherence time is given as follows:

$$T_C = \frac{1}{4B_d} \tag{2.15}$$

### 2.2.3 Delay spread

The maximum time delay in the multipath channel is known as delay spread [19], i.e. a propagation time which has been found from the difference between the longest and the

shortest path of the multipath components. The power spectrum delay profile of the channel $\phi_h(\tau)$ is used to determine the expected received power of the channel as a function of delay $\tau$ . But in practical the RMS delay spread is used instead for the absolute delay spread [6 sec. 3.6.1]. The delay spread $\tau$ is normally a short term type of fading, and the root mean square delay $\sigma_t$ is the standard deviation value of the function which expresses the maximum data rate of the channel without considering other measures such as channel equalization.
The RMS delay spread is given by:

$$\sigma_\tau^2 = \frac{\int \tau^2 \phi_h(\tau)\, d\tau}{\int \phi_h(\tau)\, d\tau} \tag{2.16}$$

It can also be expressed as root-mean-square delay $\tau_{RMS}$ as [12]:

$$\tau_{RMS} = \sqrt{\frac{\sum_{k=0}^{K-1} P_k (\tau_k - \tau_m)^2}{\sum_{k=0}^{K-1} P_k}} \tag{2.17}$$

Where we can express the average delay $\tau_m$ as:

$$\tau_m = \frac{\sum_{k=0}^{K-1} P_k \tau_k}{\sum_{k=0}^{K-1} P_k} \tag{2.18}$$

$\tau_m$ is called the multipath mean access delay time.

Where:

$\phi_h(\tau)$ : Multipath intensity profile of the channel

$P_k$ : Power of the channel $h[k]$ or delay power spectrum of the channel

The delay spread in wireless channel is given by:

$$T_d = \max_{i,j} \left| \tau_i(t) - \tau_j(t) \right| \tag{2.19}$$

### 2.2.4 Coherence bandwidth

The coherent bandwidth is a statistical measurement of the range of frequencies over the flat channel and is reciprocally related to delay spread. Coherence bandwidth has usually high correlated amplitude and phase of the multipath component. In the terms of the delay spread the coherence bandwidth is expressed as:

$$B_C = \frac{1}{2T_d} \tag{2.20}$$

Assuming that the bandwidth of the channel is much less than channel coherence

bandwidth $B_C$, and $T_d$ is maximum delay spread.

### 2.2.5 Frequency flat fading

Links which are between transmitters and receivers are usually modeled as flat fading channel in mobile wireless systems. If the symbol duration $T_S$ is longer than the delay spread $T_d$ or in another words, if the bandwidth $W$ of the input signal is less than the coherence bandwidth $B_C$, then the channel will exhibit the amplitude variation and is considered as flat fading or frequency-nonselective. This type of fading affects the amplitude and phase of the signal in the channel.

In wireless communications, the transmitted signal is typically reaching the receiver through multiple propagation paths (reflections from buildings, etc.), each having a different relative delay and amplitude. This is called multipath propagation and causes different parts of the transmitted signal spectrum to be attenuated differently, which is known as frequency-selective fading. In addition to this, due to the mobility of transmitter and/or receiver or some other time-varying characteristics of the transmission environment, the principal characteristics of the wireless channel change in time which results in time-varying fading of the received signal.

### 2.2.6 Frequency selective fading

Frequency selective fading of mobile wireless communications systems happens when multipath propagation of the signal causes different parts of the transmitted signal spectrum to be attenuated differently. When the bandwidth of the transmitted signal $W$ is much larger than the coherent bandwidth $B_C$ then the channel will suffer from inter-symbol interference, and the channel is said to be frequency selective. Similarly, when the symbol duration $T_S$ is less than the delay spread, the inter-symbol interference are created and this phenomenon occurs especially on narrow bandwidth but does not occur on wide bandwidth.

## 2.3 Previous work

Lots of works of channel modeling and simulations have been done in previous works on time-variant channel estimation. Among previous works for improving the data rate in the system are Block-Type Pilot Channel Estimation, Comb-Type Channel Estimation, inter-symbol interference (ISI) mitigation, Equalization and Iterative techniques, and Pilot arrangement or pilot-aided technique in OFDM system.

# 3. Problem definition

Testing the recently proposed method time-varying channel estimation using the Discrete Prolate Spheroidal Sequences and the Fourier basis expansion of the block length $N = 256$ symbols to model the WINNER phase II and using K, the number of basis functions for performance comparison. Investigate all three models by using just two system parameters: the Doppler bandwidth $v_{D\max}$ and the length of the data block length $N = 256$ symbols in mobile wireless communication channel at three different velocities of the user $v_{\max}$ (Both at high and low mobility). The performance of the receiver in modern mobile wireless

communication systems relies on such as the channel estimates for the time-variant frequency response $h(\tau,t)$ or as the sampled time-variant channel $h[m]$.

# 4. SYSTEM MODEL

## 4.1 The Discrete Prolate Spheroidal Sequences

The Discrete Prolate Spheroidal Sequences which has been tested in this thesis have been analyzed in a low-complexity channel estimation in a time-variant frequency-selective channel for a fully loaded multiuser multicarrier code division multiple access (MC-CDMA) downlink as shown in [2]. OFDM structures have been applied to MC-CDMA. The estimation of the time-variant channel has been done for every flat fading subcarrier with a small inter-carrier interference. The transmitted signal sequence along with known pilot symbol is applied to the system. The Doppler frequency $v_{D\max}$ depends on the carrier frequency $f_C$, the velocity of the user $v_{\max}$, and the condition of the multipath propagation [2].

## 4.2 Signal model for flat fading time-variant channel for DPSS

OFDM is used to transform the time-variant frequency-selective channel into the time-variant frequency-flat subcarriers. To avoid the inter-symbol interference between OFDM symbols, therefore the cyclic prefix is preceded. We consider the symbol sequence $x[m]$ with symbol rate $\frac{1}{T_C}$ over a flat fading time-variant channel. The symbol $T_S$ duration is much longer than the delay spread $T_d$ of the channel i.e. $T_d >> T_S$. The symbol $m$ represents the discrete time. The channel baseband equivalent is $h(\tau,t)$. The equivalent baseband represents the physical channel, transmit filter and the matched receiving filter.
The received signal $y[m]$ is given as:

$$y[m] = h[m]x[m] + z[m] \qquad m \in \{0,..., N-1\} \tag{4.1}$$

$h[m]$ : Sampled time-variant channel, which is equivalent to $h(mT,0)$
$x[m]$ : Symbol sequence
$z[m]$ : Additional circular symmetric complex white Gaussian noise with zero mean and variance $\sigma_n^2$

Where:

$$x[m] = b[m] + p[m]$$

$b[m]$ : Data symbol

$$b[m] \in \{\pm 1 \pm j\}/\sqrt{2} \qquad m \notin P$$
$$b[m] = 0 \qquad m = P$$

$p[m]$ : QPSK symbol set

$$p[m] = \{\pm 1 \pm j\}/\sqrt{2} \qquad m \in P$$
$$p[m] = 0 \qquad m \notin P$$

The pilot placement can be presented as:

$$P = \left\{ \left\lfloor i\frac{M}{J} + \frac{M}{2J} \right\rfloor \mid i \in \{0,..., J-1\} \right\} \tag{4.2}$$

For the Basis function the sequences can be written as:

$$y[m] = \underbrace{\sum_{i=o}^{D-1} u_i[m] y_i}_{h[m]} x[m] + z[m] \tag{4.3}$$

Where:

$$\begin{aligned} h[m] &= \sum_{i=0}^{D-1} u_i[m] \gamma_i \\ m &\in \{0,..., N-1\} \end{aligned} \tag{4.4}$$

Where:

$\gamma_i$ : Weight coefficient of the sequences

Therefore the estimated sequence $\tilde{h}[m]$ can be expressed as:

$$\tilde{h}[m] = \mathbf{f}^T[m]\gamma = \left( \sum_{i=0}^{D-1} u_i[m] \hat{\gamma}_i \right), \tag{4.5}$$

Where:

$$\mathbf{f}[m] = \begin{bmatrix} u_i[m] \\ . \\ . \\ . \\ u_{D-1}[m] \end{bmatrix} \in \mathbf{R}^D$$

and

$$\hat{\boldsymbol{\gamma}} = \left[ \hat{\gamma}_i, ...., \hat{\gamma}_{D-1} \right]^T \in \mathbf{C}^D$$

The Slepian basis expansion expands the sequence $h[m]$ in terms of Slepian sequences $u_i[m]$. The Slepian basis expansion can be exactly represent or replace the sampled time-variant channel $h[m]$ from the basis of Slepian sequences $u_i[m]$ as we can see from equation (4.3). The Slepian sequences $\mathbf{u}_i$ for $i \in \{0,....,5\}$ are showed in Figure 4.2. The Slepian basic expansion expands the time-variant subcarrier coefficients in term of orthogonal DPSS as explained by D. Slepian [23]. The Slepian shows that the sequence $u_i[m]$ has the maximum time concentration in a certain interval of length $N$ [2, Sec. iv],

$$\lambda(v_{D\max}, N) = \frac{\sum_{n=0}^{N-1} |u[m]|^2}{\sum_{n=-\infty}^{\infty} |u[m]|^2} \qquad 0 \le \lambda(v_{D\max}, N) \le 1 \tag{4.6}$$

Where:

$$u[m] = \int_{-v_{D\max}}^{v_{D\max}} U(v) e^{j2\pi mv} dv \tag{4.7}$$

$$U(v) = \sum_{n=-\infty}^{\infty} u[m] e^{-j2\pi mv} \tag{4.8}$$

$N$ : The block length

Which are being band-limited in the interval of $[-v_{D\max}, v_{D\max}]$.

The sequences are the eigenvectors of this eigenvalue equation:

$$\sum_{l=0}^{N-1} \frac{\sin(2\pi v_{D\max}(l-m))}{\pi(l-m)} u_i[l, v_{D\max}, N] = \lambda_i(v_{D\max} N) u_i[m, v_{D\max,} N] \tag{4.9}$$

Where:

$\lambda_i(v_{D\max}, N) u_i[m, v_{D\max}, N]$ : Eigenvalues of the concentration energy

A time concentration measure $\lambda_i$ is expressed as:

Clustered close to 1 for $i \le \lceil 2v_{D\max} N \rceil + 1$ (4.10)

and decreases rapidly to zero for $i > \lceil 2v_{D\max} N \rceil + 1$ (4.11)

The solution to constrained maximization problems (4.6), (4.7) and (4.8) is the Discrete Prolate Spheroidal Sequences. The $u_i[m, v_{D\max}, N]$ are the sequences defined as the real-valued solution of (4.9) [23].

Therefore, the Slepian sequences $\lceil 2v_{D\max} N \rceil + 1$ can enough approximate maximum time and frequency band-limited concentrated functions.

The minimum signal space dimension of time-limited snapshots of band-limited signal can be written as [23, Sec. 3.3]:

$$D' = \lceil 2v_{D\max} N \rceil + 1 \tag{4.12}$$

The condition on the signal space dimension D´ is fulfills:

$$D' \le D \le N \tag{4.13}$$

We can control the mean Square error (MSE) by choosing the dimension of the Slepian basis function $D$ i.e. the choice of $D$ can effect the MSE. The Mean Square Error is defining as:

$$MSE_N = \frac{1}{N}\sum_{m=0}^{N-1}\mathbf{E}\left\{\left|h[m]-\tilde{h}[m]\right|^2\right\} \tag{4.14}$$

Where:

$MSE_N$ : MSE of block length of $N$

The Slepian expands the sequence $h[m]$ as:

$$h[m]=\tilde{h}[m]=\sum_{i=0}^{D-1}u_i[m]\gamma_i \tag{4.15}$$

The DPSS have double orthogonality property on the infinite set $\{-\infty,....,\infty\}=\mathbf{Z}$ and the finite set $\{0,....,N-1\}$.

The sequences can be expressed in the following sense:

$$\sum_{n=0}^{N-1}u_i[m]u_j[m]=\lambda_i\sum_{-\infty}^{\infty}u_i[m]u_j[m]=\delta_{ij} \tag{4.16}$$

Where: $i,\ j\in\{0,...,N-1\}$

The Discrete Prolate Spheroidal Sequences are orthonormal on the finite set $m\in\{0,...,N-1\}$ and orthogonal on the infinite set $m\in\{-\infty,....,\infty\}$ as shown in Equation (4.16).

The Discrete Prolate Spheroid Sequence $u_i[m]$ is band-limited and has a maximum time concentration between the intervals with a sequence length $N$. The first sequence $u_0[m]$ is unique and orthogonal to all other sequences.

The Slepian sequences $u_i[m]$ can be expressed in a vector.

$$\mathbf{u}_i\in R^N \text{ with elements } u_i[m],\qquad m\in\{0,....,N-1\} \tag{4.17}$$

Now we can express the Slepian sequence $\mathbf{u}_i$ as depicted in Fig. 4.2 as the eigenvectors of matrix $\mathbf{C}$. The full expression will be as follows:

$$\mathbf{C}u_i=\lambda_i\mathbf{u}_i \tag{4.18}$$

Where matrix $\mathbf{C}\in R^{NxN}$

The eigenvalues $\lambda_i$ are the same as those in (4.9)

The matrix $\mathbf{C}$ can be defined as:

$$[\mathbf{C}]_{i,j}=\frac{\sin\left[2\pi(i-l)v_{D\max}\right]}{\pi(i-l)} \tag{4.19}$$

Where:

$$i, l \in \{0, \ldots, N-1\}$$

$[\mathbf{C}]_{i,j}$ : Value of $\mathbf{C}$ at row $i$ Column $l$

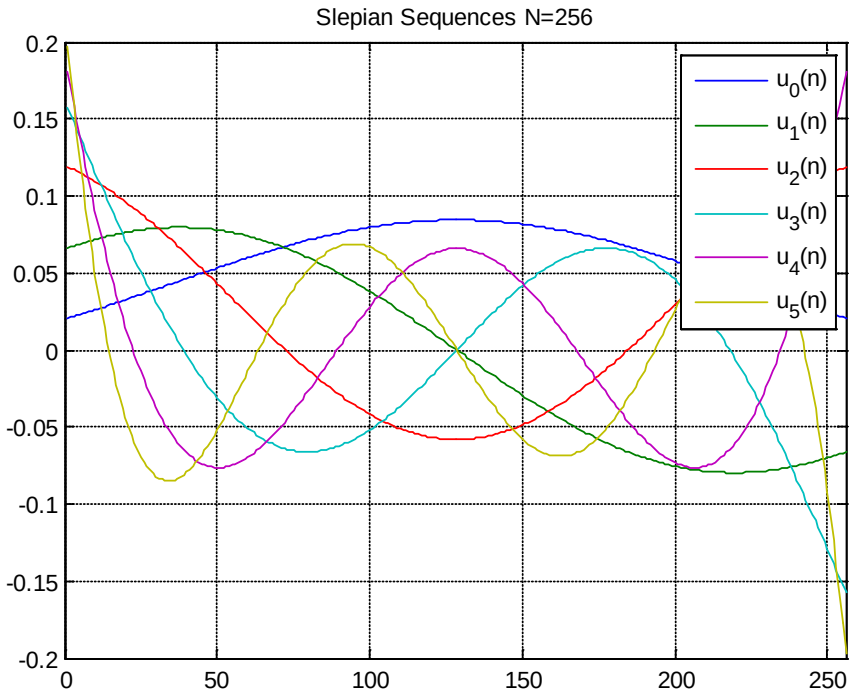


Figure 4.2 Slepian sequences $u_i[m]$ for block length $N$ = 256, D´ = 3 and $v_{D\max}$ = 0.0039.

## 4.3 Time-variant frequency-selective channel estimation

This part of the section describes the basis expansion for time-variant frequency-selective channel estimation in a MC-CMDA downlink in a low complexity algorithm which based on OFDM applied to the generalized finite Slepian basis expansion on a per-subcarrier basis. The assumption of the wireless channel estimation is based on the maximum normalized one-sided Doppler bandwidth as shown in Equation (1.3)

$$v_{D\max} = \frac{v_{\max} f_C}{c_0} T_S \geq \left| f_l T_S \right|, \tag{4.20}$$

Where:

$v_{D\max}$ : Maximum supported velocity
$T_S$ : Symbol duration
$c_0$ : Speed of light
$f_C$ : Carrier frequency
$f_l$ : Doppler shift of the component $l$

As we know that the performance of the receiver depends on the accurately estimate of the time-variant frequency response $g[m] \in \mathbf{C}^N$.
The MC-CDMA signal model over N parallel frequency-flat channel is expressed as:

$$y[m,q] = g[m,q]x[m,q] + z[m,q], \tag{4.21}$$

Where:

| | |
|---|---|
| $q$ | : Set of equation for every subcarrier $q \in \{0,....,N-1\}$ |
| $g[m,q]$ | : Time-variant frequency-flat subcarrier |
| $x[m,q]$ | : Elements of $x[m]$. $x[m]$ is the transmitted symbol at time index $m$ |
| $h[m,n]$ | : Time-variant impulse response of elements of $h[m]$ |
| $z[m,q]$ | : White Gaussian noise at time $m$ for subcarrier $q$ |

The index $q$ is omitted if a subcarrier is fixed and Equation (4.21) will become:

$$y[m] = g[m]x[m] + z[m] \tag{4.22}$$

The band-limited property of $h[m,n]$ directly applies to $g[m,q]$ as well and it allows us to estimate the time-variant frequency-flat subcarrier $g[m,n]$ with the Slepian basis expansion and we define:

$$\hat{\boldsymbol{\psi}}_i[q] = \frac{1}{\sum_{m \in p} \left| u_i[m]\, p[m,q] \right|^2} \sum_{m \in p} y[m,q]\, p[m,q] u_i[m], \tag{4.23}$$

Where $\hat{\boldsymbol{\psi}}[q] = \left[ \hat{\psi}_0[q], ...., \hat{\psi}_{(D-1)}[q] \right]^T$, $i \in \{o,....,D-1\}$ and $q \in \{o,....,N-1\}$
The estimated time-variant frequency response is expressed as [12]:

$$\tilde{q}[m,q] = \sum_{i=0}^{D-1} u_i[m] \hat{\psi}_i[q] \tag{4.24}$$

To obtain the noise suppression is by exploit the correlation between the sub-carriers:

$$\hat{\mathbf{g}}[m] = \mathbf{F}_{NxL} \mathbf{F}_{NxL}^H \tilde{\mathbf{g}}[m]. \tag{4.25}$$

Where:

$$\left[ \mathbf{F}_N \right]_{i,l} = e^{-j2\pi il/N}$$

The channel estimates $\hat{g}[m]$ and insert into the time-variant effective spreading sequences is defined as:

$$\tilde{\mathbf{s}}_k[m] = diag\left(\mathbf{g}[m]\right)\mathbf{s}_k . \tag{4.26}$$

Where:

$\mathbf{s}_k$ : Spreading matrix $\mathbf{S}$, $k \in \{1,....,K\}$

The time-variant effective spreading in matrix form is given by:

$$\tilde{\mathbf{S}}[m] = \left[\tilde{\mathbf{s}}_1[m],....,\tilde{\mathbf{s}}_K[m]\right] \in \mathbf{C}^{NxK} \tag{4.27}$$

The time-variant multi-user detector performs when the linear MMSE receiver detects the data using the received vector $\mathbf{y}[m]$ as in Equation (4.1), the spreading matrix $S$, and the time-variant frequency response $\mathbf{g}[m]$.

## 4.4 Fourier Basis Expansion

The Fourier basis expansion is defined as:

$$h[m] = \sum_{i=0}^{D-1} \gamma_i u_i[m], \qquad m \in \{0,...., N-1\} \tag{4.28}$$

Where:

$$u_i[m] = \frac{1}{\sqrt{N}} e^{(j2\pi(i-(D-1)/2)m/N)} \tag{4.29}$$

$\gamma_i$ : Weight coefficient of the sequences

Where Equation (4.28) define the basis expansions for $i \in \{0,...., D-1\}$ and

$$\lceil 2\nu_{D\max} N \rceil + 1 \le D \le N-1 \tag{4.30}$$

The generic notation for the basis expansion quantities such as:
$u_i[m]$, $D$, $\gamma_i$ and $\tilde{h}[m]$ are applicable to any set of orthogonal basis functions $u_i[m]$.
We can determine the basis expansion parameters depending on [12] according to

$$\gamma_i = \sum_{n=0}^{N-1} h[m] u_i[m], \; i \in \{0,...., D-1\} \tag{4.31}$$

The channel spreading function for Fourier basis function is given as:

$$S_{\mathbf{H}}(\nu) = \sum_{m=-\infty}^{\infty} h[m] e^{-j2\pi m\nu}, \quad -1/2 \le \nu < 1/2 \tag{4.32}$$

If maximum normalized Doppler bandwidth $\nu_{D\max}$ in wireless system is known, so the channel spread $S_{\mathbf{H}}$ is band-limited and will vanish for $|\nu| > \nu_{D\max}$.

Now we can express the time-variant channel as:

$$h[m] = \int_{-v_{D\max}}^{v_{D\max}} S_{\mathbf{H}}(v) e^{j2\pi m v} dv \tag{4.33}$$

Simulations of the Fourier basis expansion

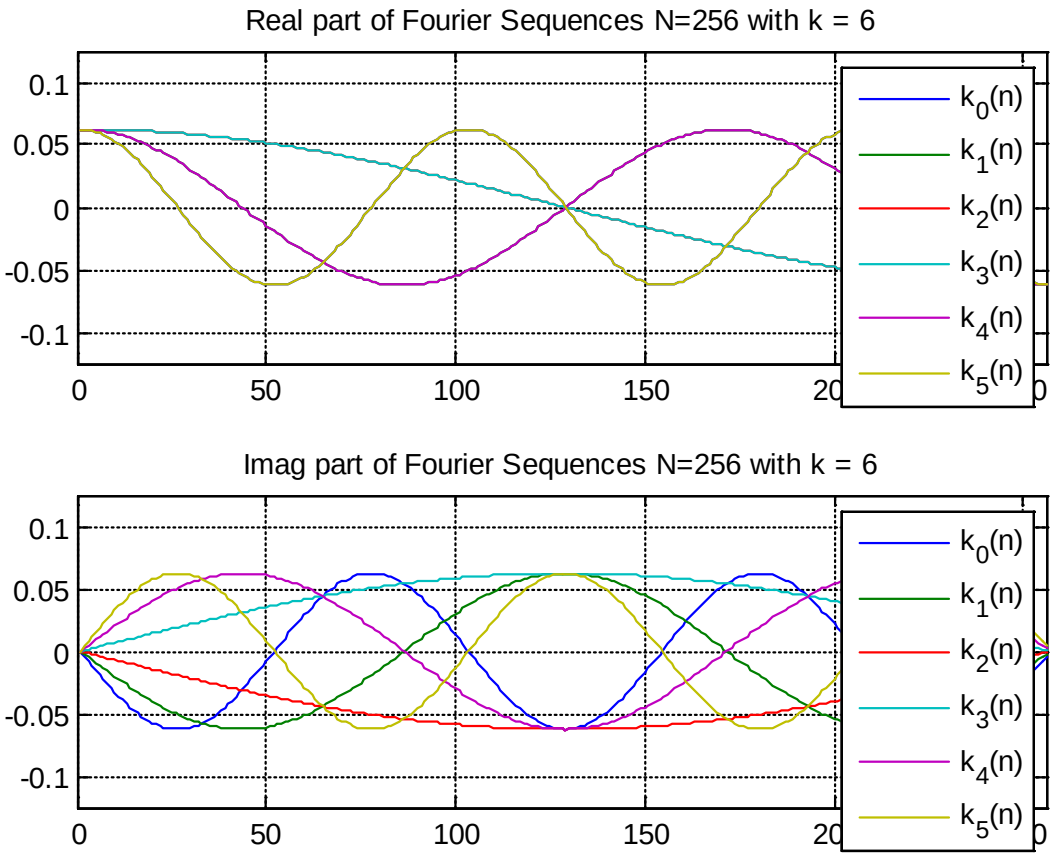


Figure 4.4 Fourier Basis Expansion $k_i[n]$ as a function of sequences of $n$

## 4.5 System model for WINNER model

The mobile communication channel of the WINNER model uses MIMO system for both the transmitter and the receiver and only single radio link is used in this thesis. MIMO employs multiple antennas at the transmitter and receivers to open up additional sub-channels in spatial domain. The antenna is 3D Antenna array which provides the polarization directional filtering and spatial displacement. The mobile is situated ca. 50 meters away from the Base Station; the WINNER model covers the minimum radius of 10 meters and the maximum radius of 500 meters. The shadow fading model applied is Rayleigh distribution with $\sigma = 8$ dB, assuming that the mobile is situated in typical urban envelopment (TU). The WINNER model generates the time-variant channel impulse responses (CIR).

## 4.6 Channel model for WINNER model

The WINNER II channel model has two sets parameters: the large scale (LS) and the small scale. For the large scale parameters, such as shadow fading, delay and angular spreads which are fixed to median values but angle remains randomly from tabulated distribution functions. Meanwhile the small scale parameters such as delays, power and directions of angle of arrival and departure are randomly according to tabulated distribution functions. We say large scale (LS) when the distance of channel segment is of some tens of wave lengths. All propagation parameters are frozen in order to model Clustered Delay Line (CDL). The correlation matrices are obtained from CDL model by fixing the antenna structure. The CDL model has clusters with fixed number of 20 rays (sub-paths) each as in 3PP Spatial Channel Model (SCM). A cluster constitutes of a number of rays. The CDL model explains the propagation channel which has a different number of multipath component clusters with different delays and they always differ in angle of departure and arrival. [See Table C.2.3 in the Appendix].
The WINNER II channel model uses OFDM technique. The channel model uses 100 MHz Radio frequency bandwidth. Two strongest clusters are divided into three sub-clusters and only polarized arrays are used. The velocity of the Mobile is 28.5 m/s (102.6 km/h), the centre frequency set to 2.0 GHz, the sample frequency of the channel $f_S = \frac{1}{T_S}$ is 43.6 MHz and the sampling time is $\frac{1}{f_S}$. Furthermore, the delay sampling interval has been set to $5.0*10^{-9}$. The Winner II channel model uses 500 meters maximum radii for macro-cell [28].
The generation of channel coefficients for each cluster in the WINNER II model is given as follows:

$$\mathbf{H}_{u,s,n}(t) = \sqrt{P_n}\sum_{n=1}^{N}\begin{bmatrix} F_{tx,s,Y}(\phi_{n,m}) \\ F_{tx,s,H}(\phi_{n,m}) \end{bmatrix}^T \begin{bmatrix} \exp(j\Phi_{n,m}^{vv}) & \sqrt{K_{n,m}}\exp(j\Phi_{n,m}^{vh}) \\ \sqrt{K_{n,m}}\exp(j\Phi_{n,m}^{hv}) & \exp(j\Phi_{n,m}^{hh}) \end{bmatrix} \begin{bmatrix} F_{rx,u,Y}(\varphi_{n,m}) \\ F_{rx,u,H}(\varphi_{n,m}) \end{bmatrix} \quad (4.34)$$

$$* \exp\left(jd_s 2\pi\lambda_o^{-1}\sin(\phi_{n,m})\right)\exp\left(jd_u 2\pi\lambda_o^{-1}\sin(\varphi_{n,m})\right)\exp(j2\pi\nu_{n.m}t)$$

$F_{rx,u,V}$ : The antenna element u field pattern for vertical polarization

$F_{rx,u,H}$ : The antenna element u field pattern for horizontal polarization

$d_s$ : The uniform distance in meters between transmitter and receiver element

$d_u$ : The uniform distance in meters between transmitter and receiver element

$\lambda_o$ : The wavelength on carrier frequency.

$\exp(j\Phi_{n,m})$ : The scalar is equivalent to 2x2 polarization matrix

$\nu_{n,m}$ : Doppler frequency component

$K_{n,m}$ : Rician K-factor

$\Phi_{n,m}$ : Random initial phase for each ray m of each cluster n

and four different polarizations (vv, vh, hv, hh)

$\phi_{n,m}$ : Departure angle unit of ray n, m

$\varphi_{n,m}$ : Arrival azimuth angle unit of ray n, m

The channel links level has been broken down into three types of parameters, the big scale, the medium scale and the small scale parameters. In the WINNER model the large scale parameters are fixed. The large scale propagation model is the model which takes the average received power of the path loss over longer distance between the Base Station and Mobile Station. Small scale parameters are usually used on multipath channel and the parameters are about equal to value of the wavelength of the fading signal.
The WINNER model was used in urban environment C2 (typical urban (TU)) macro-cell [see Appendix C.2.1]. The model uses a Rayleigh channel model, i.e. Non line of sight (NLOS) scenario model and it is homogeneous in the propagation conditions. The NLOS has Delay spread (DS) of 234 ns, Azimuth Spread (AS) at the Base Station of $8^o$ and Azimuth Spread at Mobile Station of $53^o$ and the shadow fading $\sigma = 8$ dB [28].

The path loss of the C2 NLOS is given by:

$$P_{NLOS} = (44.9 - 6.55\log_{10}(h_{BS}))\log_{10}(d) + 34.46 + 5.83\log_{10}(h_{BS}) + 23\log_{10}(f_c / 5.0) \quad (4.35)$$

Where:

$h_{BS}$ : The Base Station antenna height with 25 m and $h_{MS}$ = 1.5 m high

$f_c$ : The center carrier frequency or the system frequency in GHz

$d$ : The distance between the transmitter and the receiver with the range of between 50 m and 5 km

The path loss for C2 of Winner model is expressed as:

$$P_{LOS} = 40.0l0g_{10}(d) + 13.47 - 14.0\log(h_{BS}) - 14.0\log_{10}(h_{MS}) + 6.0\log_{10}(f_c / 5.0) \quad (4.36)$$

With shadow fading $\sigma = 6$ dB.

Where:

$h_{MS}$ : The antenna height of Mobile Station

# 5 Power Spectrum Estimation

This thesis uses the Power spectrum of the WINNER channel in order to determine and investigate the Doppler frequency of the time-variant channel. Before proceeding, the power spectrum estimation of the channel is briefly explained. Estimating of the sequence of time samples of the transmitted random signal is the same as estimating the power spectrum of the transmitted signal. Estimating the power spectrum is equivalent to estimating the autocorrelation. The Power spectrum helps us to understand the long term behavior of transmitted signal by taking the Fourier transform of the signal. Power spectrum explains the distribution of the power contained in the transmitted signal and Power spectrum measures the

frequency content of stochastic process. The spectrum estimation is divided into two types: parametric and nonparametric. There are many different types of techniques used for power estimating, but in this thesis the periodogram, which is non-parametric method is used.

## 5.1 The Periodogram

The estimate of the power spectrum of Wide-Sense Stationary (WSS) random process is done by taking the Fourier transform of the autocorrelation sequences. Arthur Schuster is the first one to explain for his study of periodicities in sunspot in 1898 about the Periodogram as an estimate of the power spectrum of a signal. The problems of periodogram are concerned with limits and accuracy when estimating the power spectrum, especially for short data records. There are other methods used to improve the power spectrum by forming smoothing and averaging such as Bartley, Blackman-Turkey and Welch methods.
The Power spectrum is given by:

$$P_x\left(e^{jw}\right)=\sum_{k=-\infty}^{\infty} r_x(k)e^{-jkw} \tag{5.1}$$

Where:

$$r_x(k)=\frac{1}{N}\sum_{n=0}^{N-1-k} x(n+k)x^*(n) \quad k=\{0,1,.....,N-1\} \tag{5.2}$$

We can rewrite the periodogram as:

$$\hat{P}_x\left(e^{jw}\right)=\sum_{k=-N+1}^{N-1}\hat{r}_x(k)e^{-jkw}=\hat{P}_x(f)=\frac{1}{N}\left|\sum_{k=0}^{N-1}x(k)e^{-j2\pi fk}\right|^2=\frac{1}{N}\left|F\left\{x_N(k)\right\}\right|^2 \tag{5.3}$$

Where:

$F$ : Fourier transform

: $w=2\pi f$

The process $x(k)$ has a finite length signal interval [0,1…..,N-1]

## 5.2 Periodogram with Rectangular window

In order to view the power spectrum of the WINNER model, the rectangular window is used. The rectangular window is an amplitude weight for truncating continuous time signal to fit within the length of DFT window. The rectangular window has a value of 1 over the length of the window and zero outside [16]. The rectangular window has larger sidelobes which lead to masking of weak narrowband components, and it has the least amount of spectral smoothing. Using convolution theorem, the periodogram is given by:

$$\hat{P}_x\left(e^{jw}\right)=\frac{1}{N}X_N\left(e^{jw}\right)X_N^*\left(e^{jw}\right)=\frac{1}{N}\left|X_N\left(e^{jw}\right)\right|^2 \tag{5.4}$$

Where:

$X_N\left(e^{jw}\right)$ : The discrete-time Fourier transform of the N-point data sequence $x_N(n)$.

The discrete Fourier transform of sequence $x_N(n)$ can be expressed as:

$$X_N(e^{jw}) = \sum_{n=-\infty}^{\infty} x_N(n) e^{-jnw} = \sum_{n=0}^{N-1} x_N(n) e^{-jnw} \tag{5.5}$$

Where:

$$x_N(n) = w_R(n) x(n) \tag{5.6}$$

The Fourier transform of rectangular window $w_R(n)$ is given as:

$$W_R(e^{jw}) = \frac{\sin(Nw/2)}{\sin(w/2)} e^{-j(N-1)w/2} \tag{5.7}$$

To make the periodogram easier for computing the DFT, the expression can be written as:

$$x_N(n) \underline{DFT} X_N(k) \rightarrow \frac{1}{N} \left| X_N(k) \right|^2 = P_{per}\left(e^{j2\pi k/N}\right) \tag{5.8}$$

The resolution of the periodogram is given by:

$$\mathrm{Re}\, s\left[\hat{P}(e^{jw})\right] = 0.89 \frac{2\pi}{L} \tag{5.9}$$

## 6. Simulation results and analysis

All evaluations and simulations have been implemented by Matlab.
Here are the results of the calculation of DPSS parameters;
The calculation for one-sided normalized maximum Doppler bandwidth is as follows:

$$v_{D\max} = \frac{v_{\max} f_C}{c_o} T_S = 0.0039 \tag{6.1}$$

Where:

The maximum velocity of the user $v_{\max}$: 28.5 m/s = 102.6 km/h
The carrier center frequency $f_C$: 2 GHz
The Block length $N$: 256 symbols
The minimum signal space dimension $D' = \lceil 2 v_{D\max} N \rceil + 1$: 3
The speed of light $c_0$: $2.99792458*10^8$
The symbol rate $1/T_S$: $48.6*10^3\ s^{-1}$

## 6.1 WINNER phase II model

For simulation of the power spectrum of the WINNER model, the first step is to estimate the

autocorrelation sequences function $R_{XX}$ and then to apply the Fourier transform of the sequences. This is followed by using periodogram, a nonparametric method with the DTFT of a rectangular window $w_R(n)$ together with zero padding in order to improve the resolution in the results when using FFT. Figure 6.1 shows the Base Station (BS) in red, the link in dark blue together with the Mobile Station (MS) in blue, which is situated 50 meters far away from BS and moves at the velocity of 102.6 Km/h towards south west. The number of the samples of the channel (Data length) $N$ is 256*32 = 8192, number of FFT coefficients is 8000, length of Window is 8000, and the sample frequency of the channel $f_S = \frac{1}{T_S}$ is $48.6*10^3$ Hz. The Blackman window – sidelobe suppression (-58 dB) has been applied.

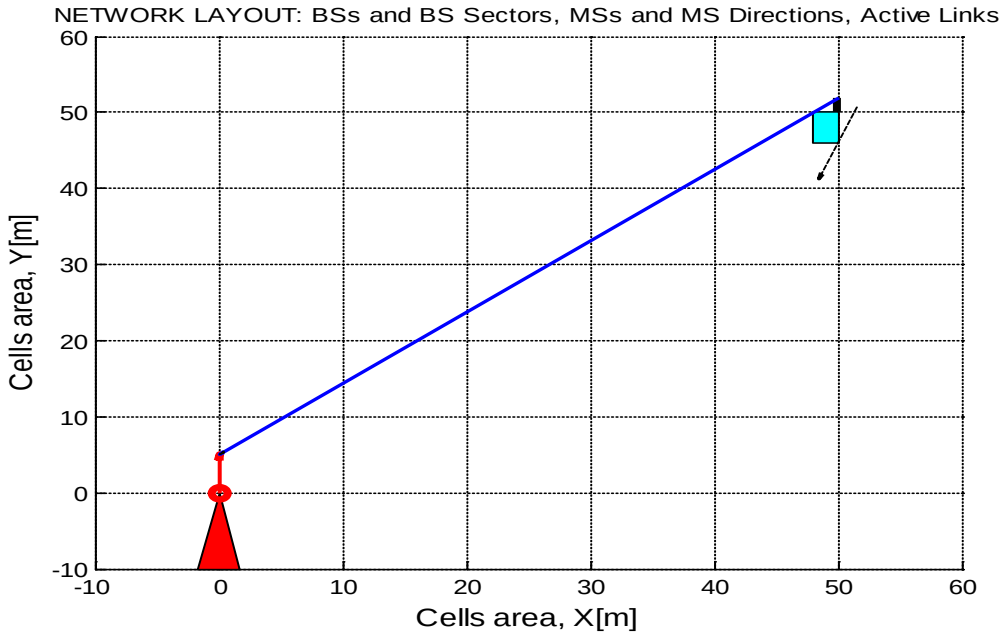


Figure 6.1 BS, MS, active link and direction of the MS

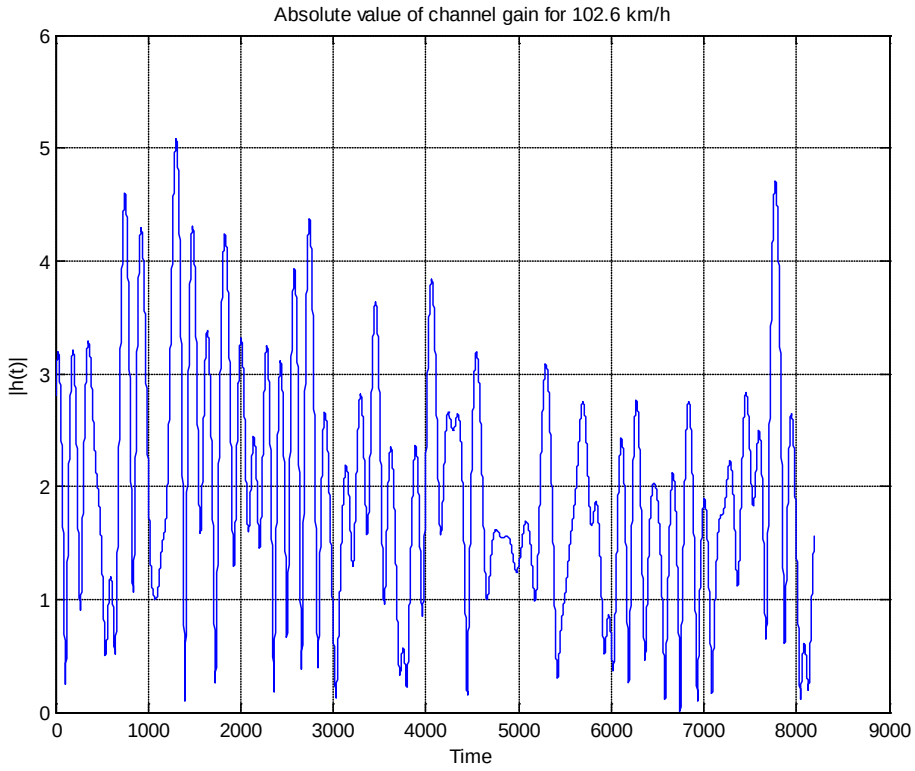


Figure 6.2 Channel gain as a function of time at 102.6 km/h

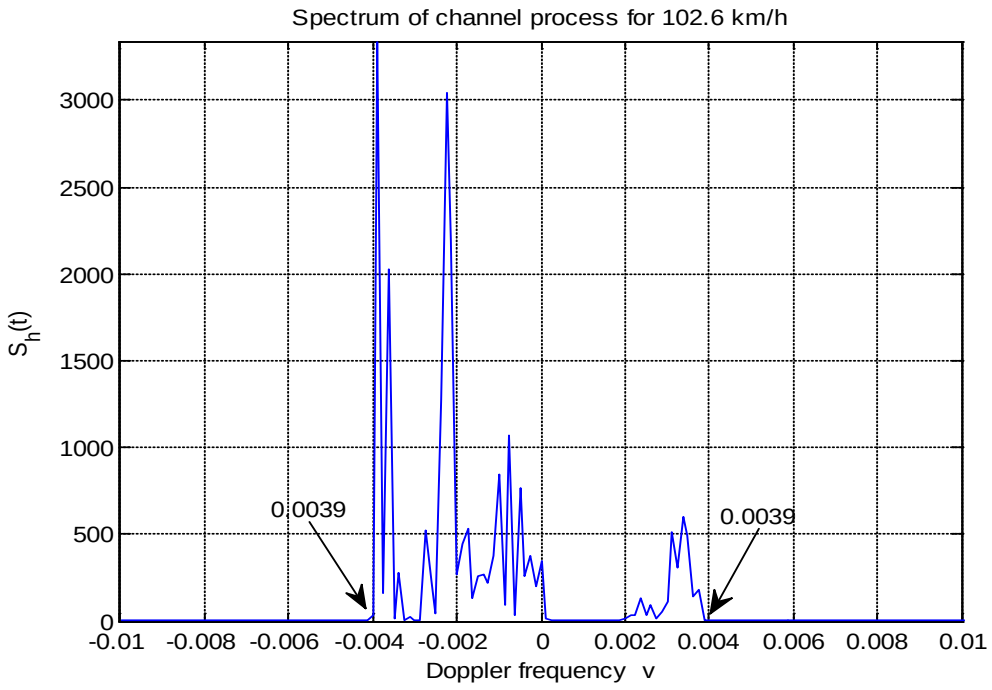


Figure 6.3 Power spectrum of channel process as a function of normalized Doppler frequency $\nu$ in a high mobility at 102.6 km/h and $\nu_{D\max}$ = 0.0039

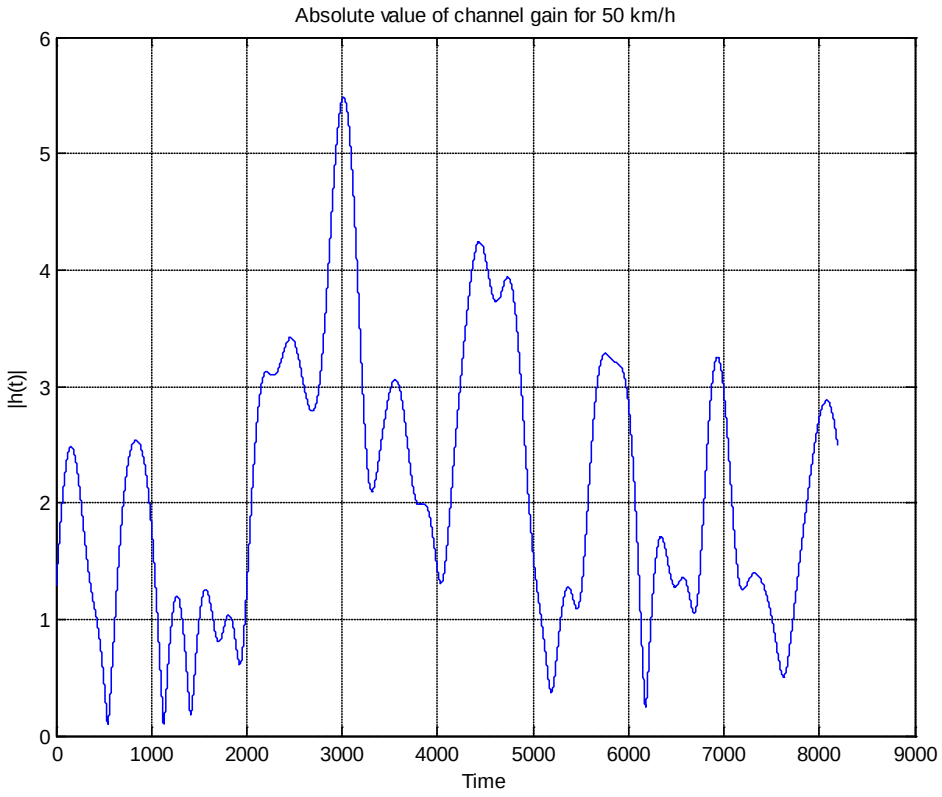


Figure 6.4 Channel gain as a function of time at 50 km/h

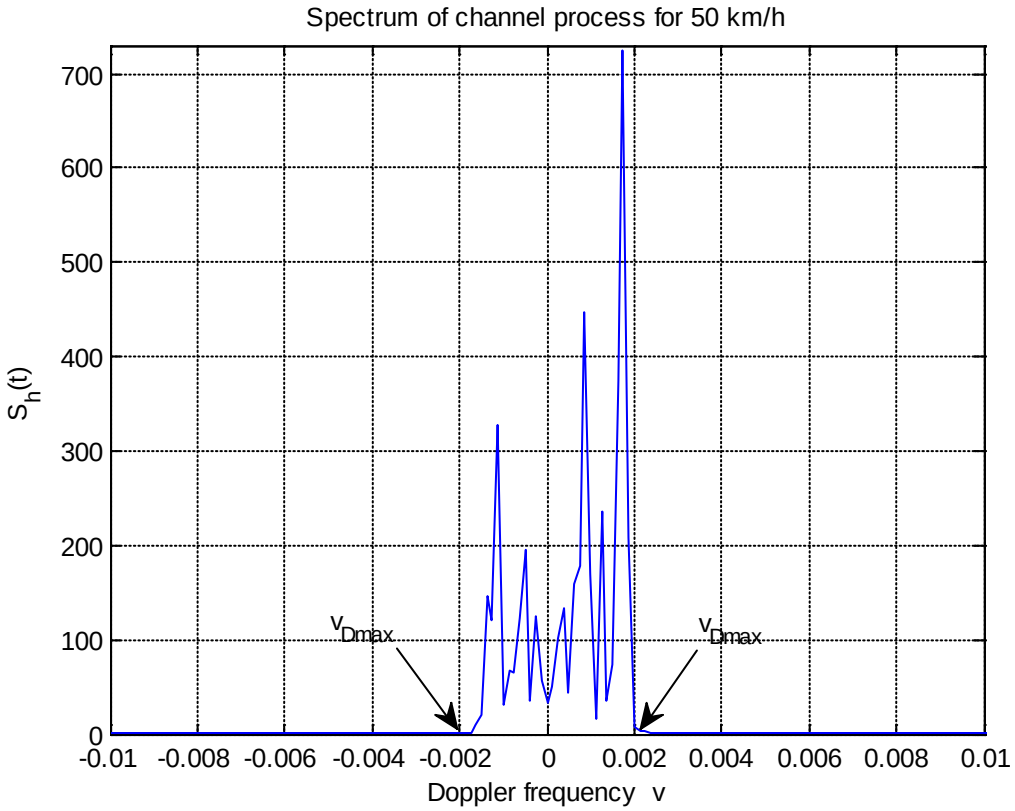


Figure 6.5 Power spectrum of channel process as a function of normalized Doppler frequency $v$ at 50 km/h and $v_{D\max} = 0.0019$

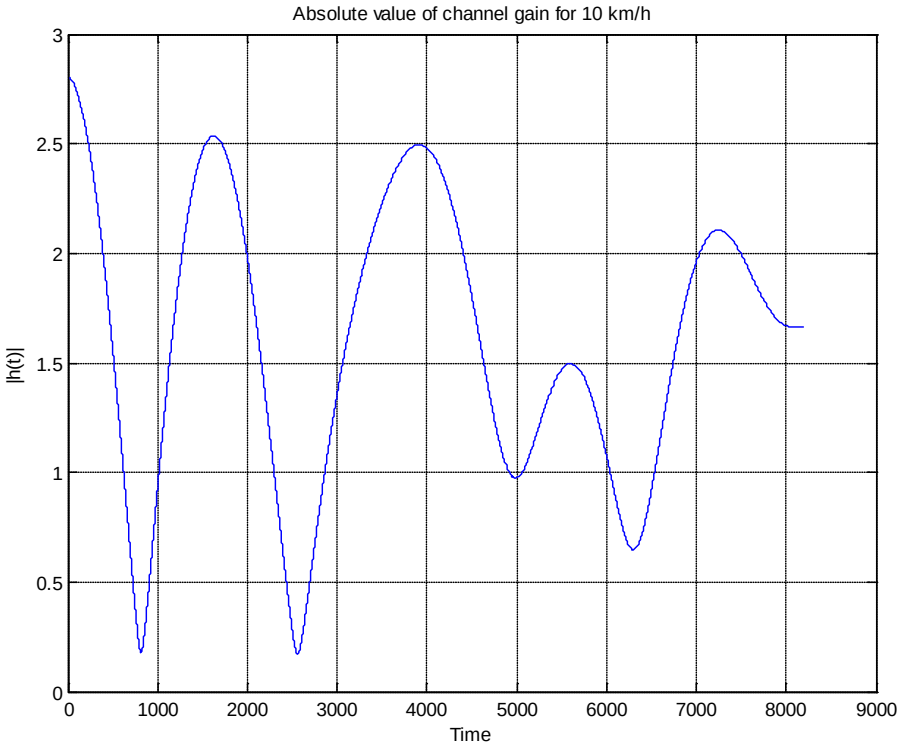


Figure 6.6 Channel gain as a function of time for a low mobility at 10 km/h

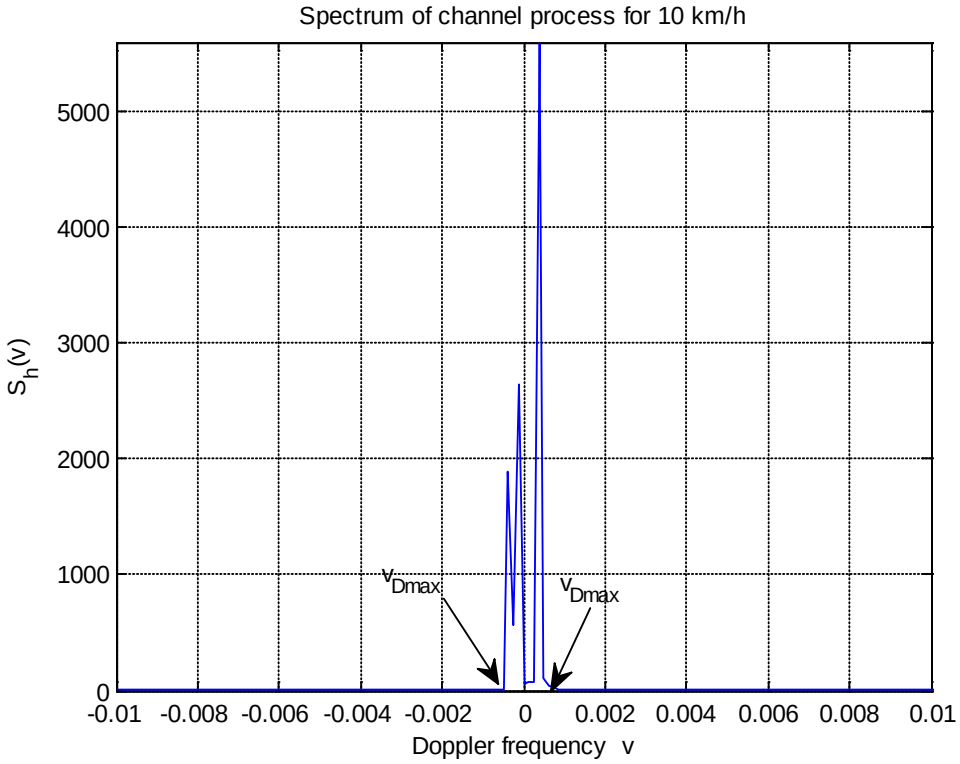


Figure 6.7 Power spectrum of channel process as a function of normalized Doppler frequency $v$ in a low mobility at 10 km/h and $v_{D\max} = 3.8*10^{-4}$

The result of the power spectrum of the channel process caused for WINNER model has exactly the same value of the one-sided normalized Doppler frequency of 0.0039 as in Discrete Prolate Spheroidal Sequences.
The scenario parameters of simulation are set as follows:

- Number of the samples of the channel $N$ = 8192 [To get better resolution]
- Speed of light $c_o = 2.99792458*10^8$
- Centre frequency $f_C$ = 2 GHz
- Sample frequency of the channel $f_S = \frac{1}{T_S} = 48.6*10^3$ Hz
- Sampling time $T_S = \frac{1}{f_S} = 1/48.6*10^3$ S
- Propagation condition = Non line of sight (NLOS)

## 6.2 Simulation of the channel estimation of the WINNER II channel model, Slepian basis expansion and Fourier basis expansion

The following are the simulations obtained from the channel which is so close to the true channel as possible i.e. accurate and realistic one. The channel model is selected as a typical urban (TU) scenario modeled by Spatial Channel Model Extended (SCME) of the WINNER phase II model, which generates the channel impulse response $h[\tau, t] = h[m]$ based on the 3GPP long term evolution (LTE) channel model specifications with a symbol rate $f_S = \frac{1}{T_S} = 48.6*10^3 s^{-1}$, a sampling time $2.0576*10^{-5}$ and the system operates at carrier frequency $f_C = 2$ GHz. The system is design for three different velocities $v_{\max}$: 102.6 km/h, 50 km/h, and 10 km/h. The channel model is a typical urban scenario with Non line of sight (NLOS) as propagation scenario. The WINNER II channel model is then compared to Slepian basis expansion and as well as Fourier basis expansion with the data block length $N$ = 256 i.e. the number of samples of the channel.

### 6.2.1 Simulations of the channel estimation of the WINNER II model and the Slepian basis expansion

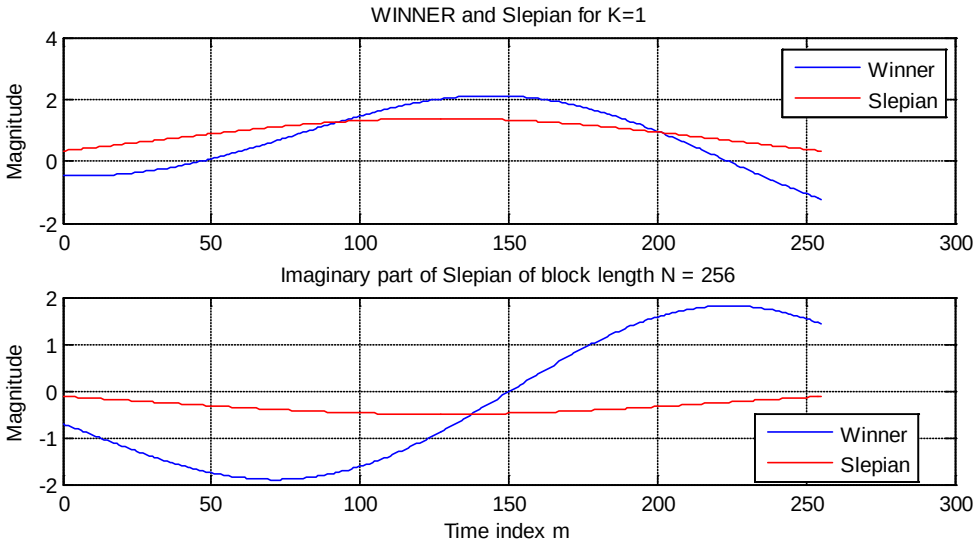


(a)

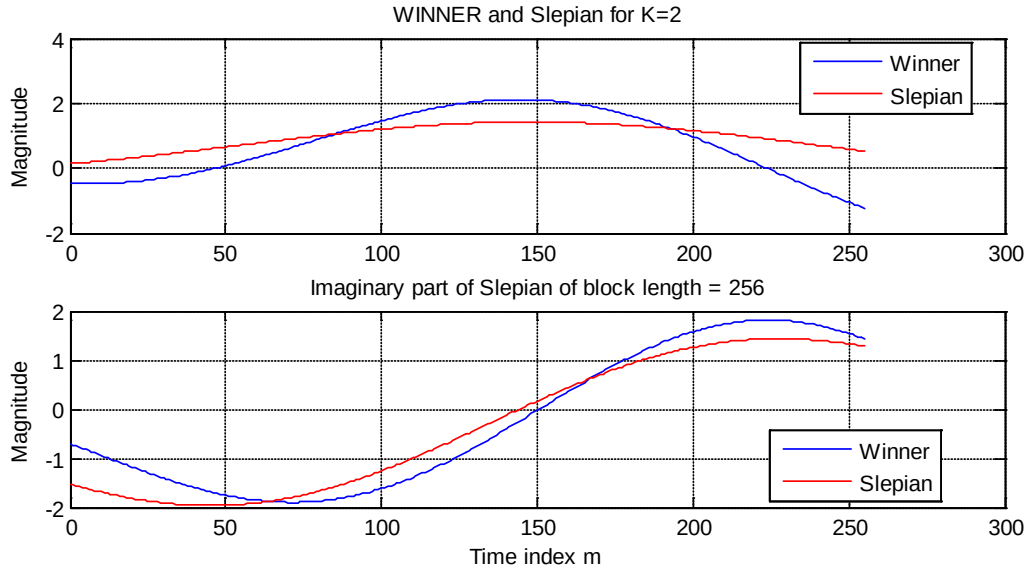


(b)

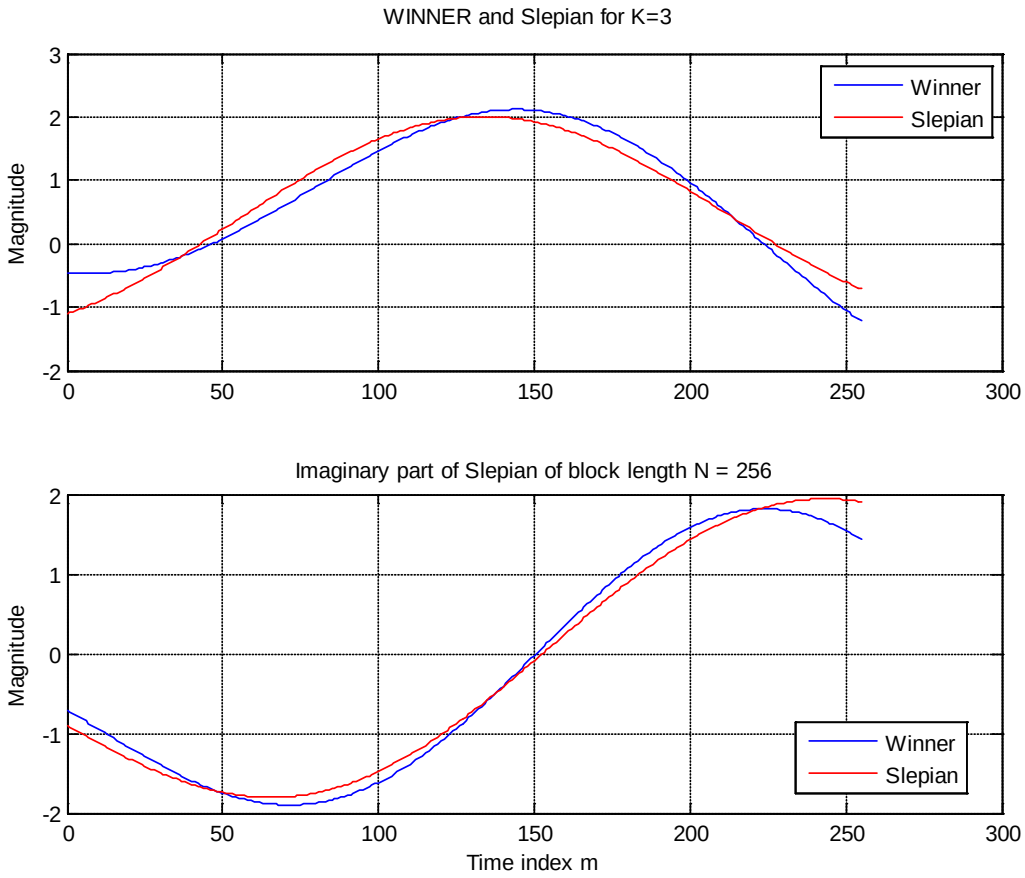
WINNER and Slepian for K=3
Magnitude
Winner
Slepian
Imaginary part of Slepian of block length N = 256
Magnitude
Winner
Slepian
Time index m

(c)

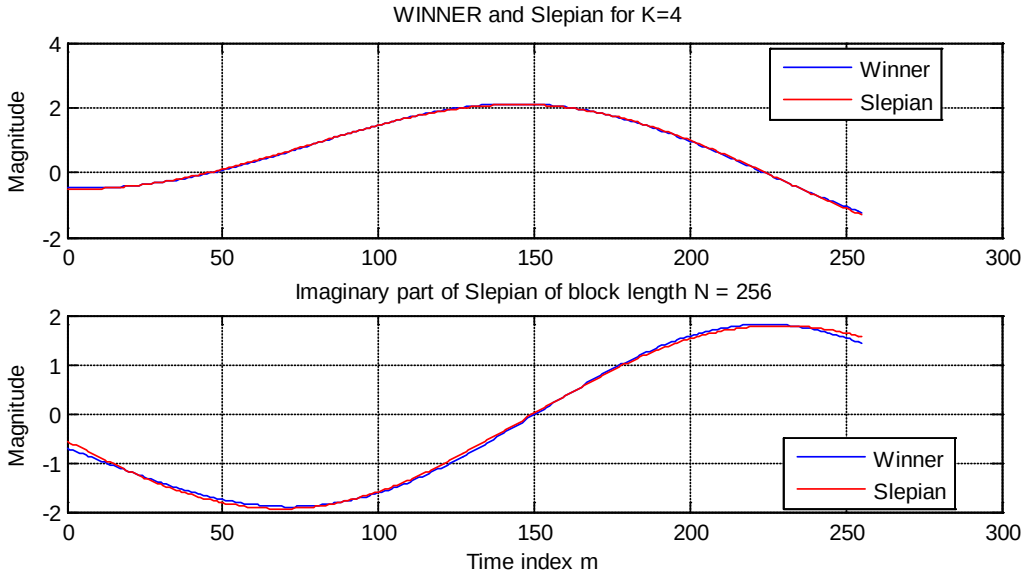
WINNER and Slepian for K=4
Magnitude
Winner
Slepian
Imaginary part of Slepian of block length N = 256
Magnitude
Winner
Slepian
Time index m

(d)

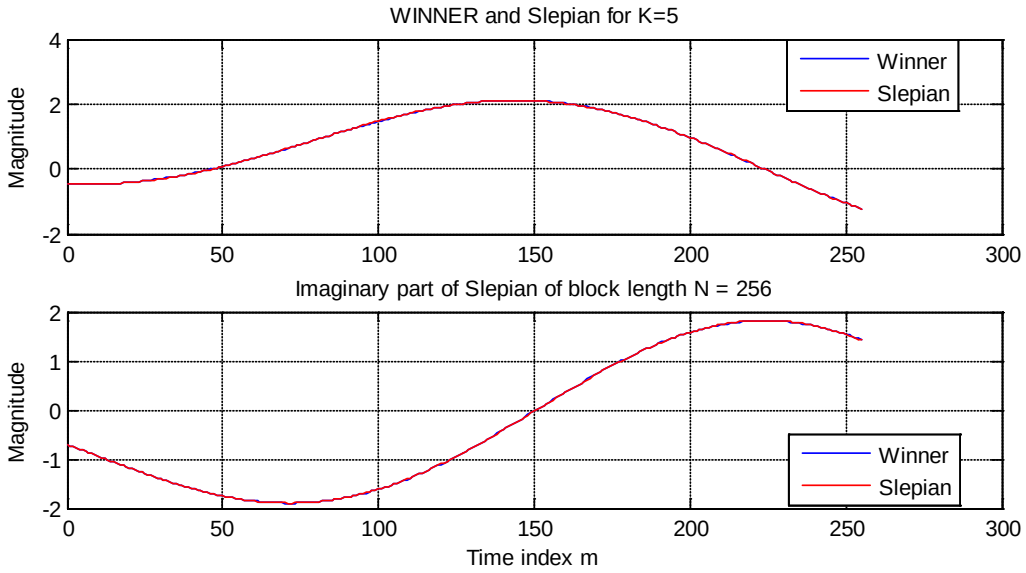


(e)

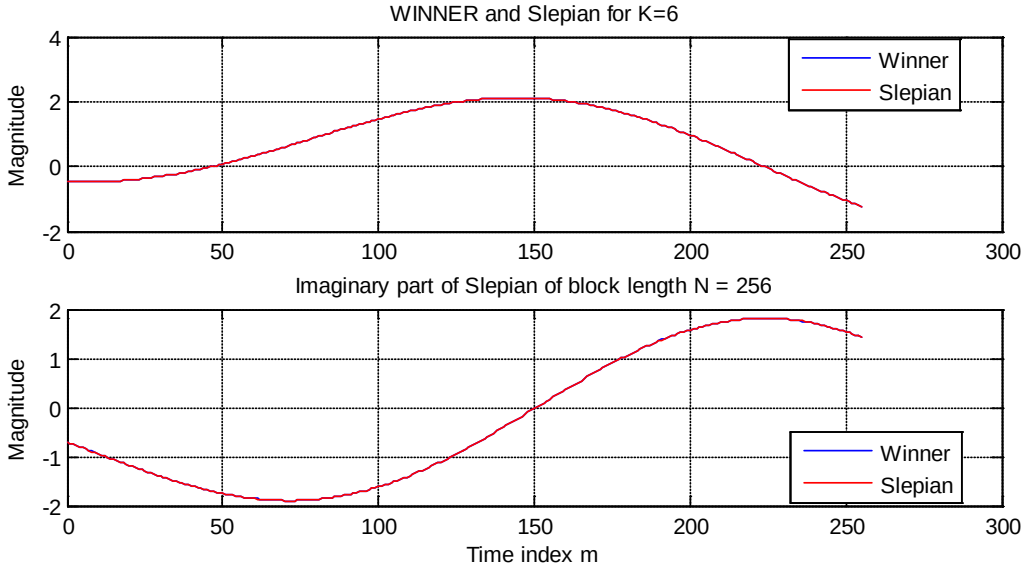


(f)

Figure 6.8 The fitting of WINNER model with Slepian basis expansion as a function of time index *m*
a) For N = 256 and K = 1 b) For N = 256 and K = 2 c) For N = 256 and K = 3 d) N = 256 and K = 4 e) For N = 256 and K = 5 f) For N = 256 and K = 6

### 6.2.2 Simulations of the channel estimation of the WINNER II model and the Fourier basis expansion

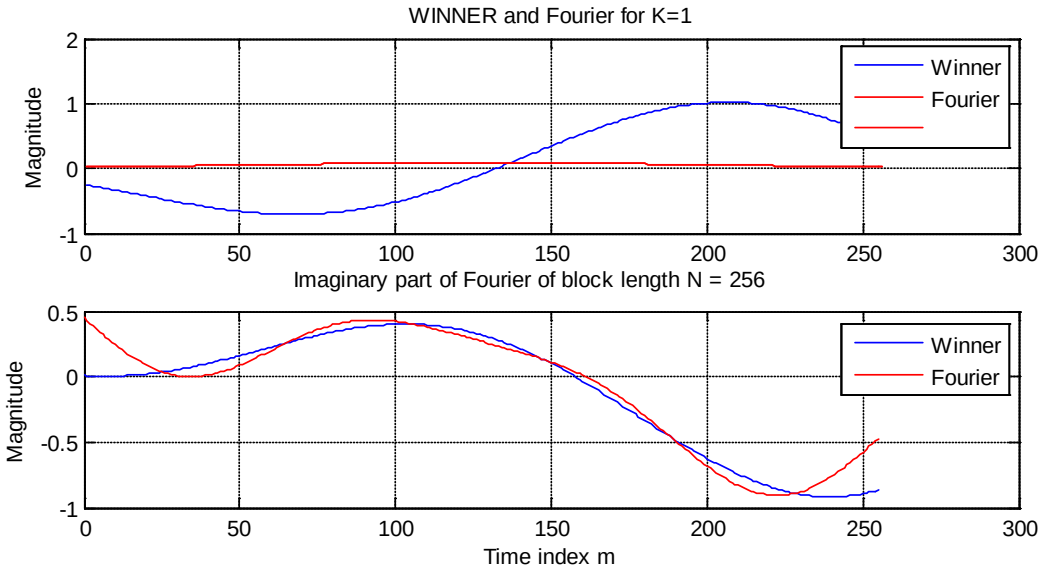


(a)

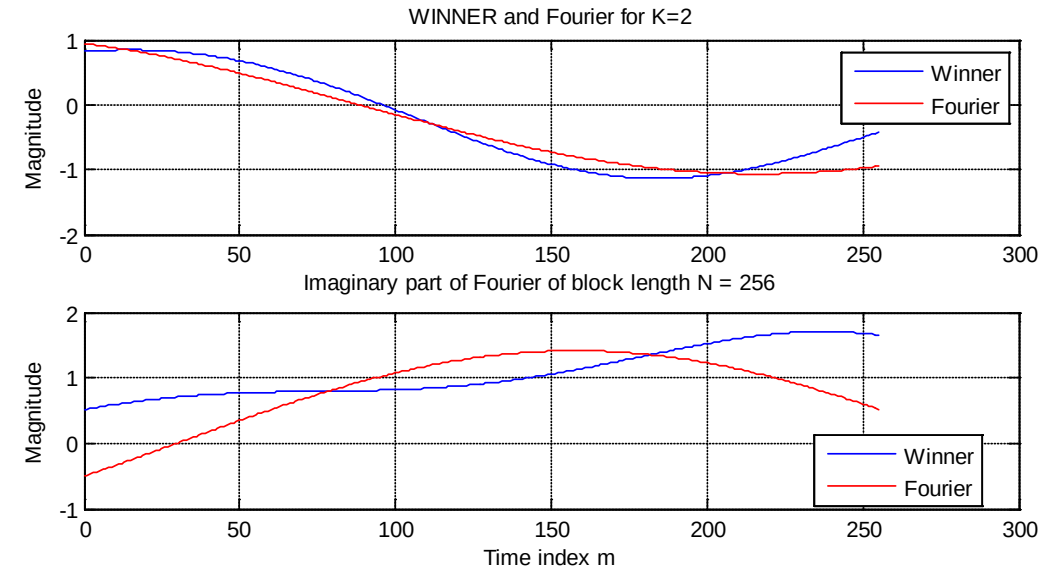


(b)

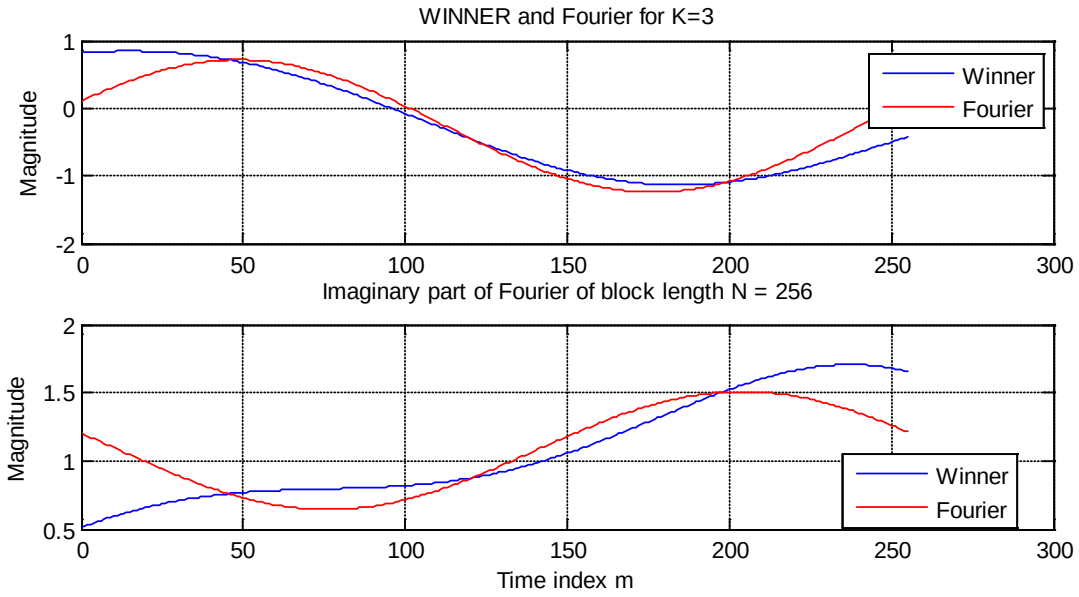
WINNER and Fourier for K=3
Magnitude
Winner
Fourier
Imaginary part of Fourier of block length N = 256
Magnitude
Winner
Fourier
Time index m

(c)

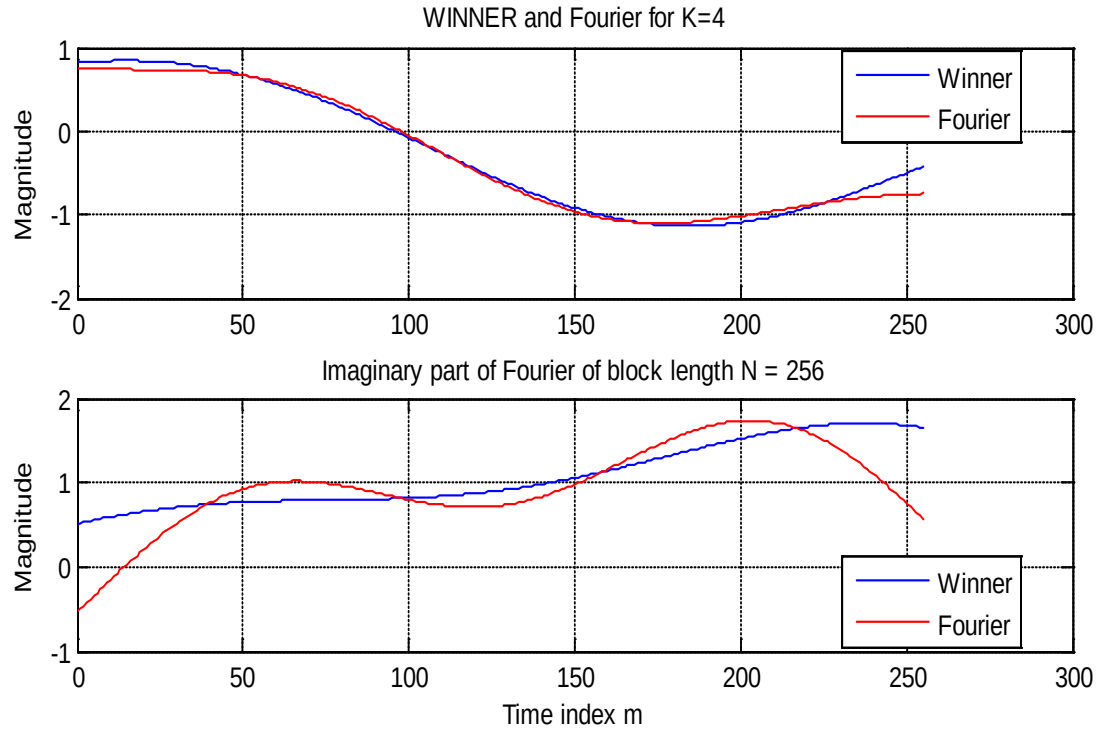
WINNER and Fourier for K=4
Magnitude
Winner
Fourier
Imaginary part of Fourier of block length N = 256
Magnitude
Winner
Fourier
Time index m

(d)

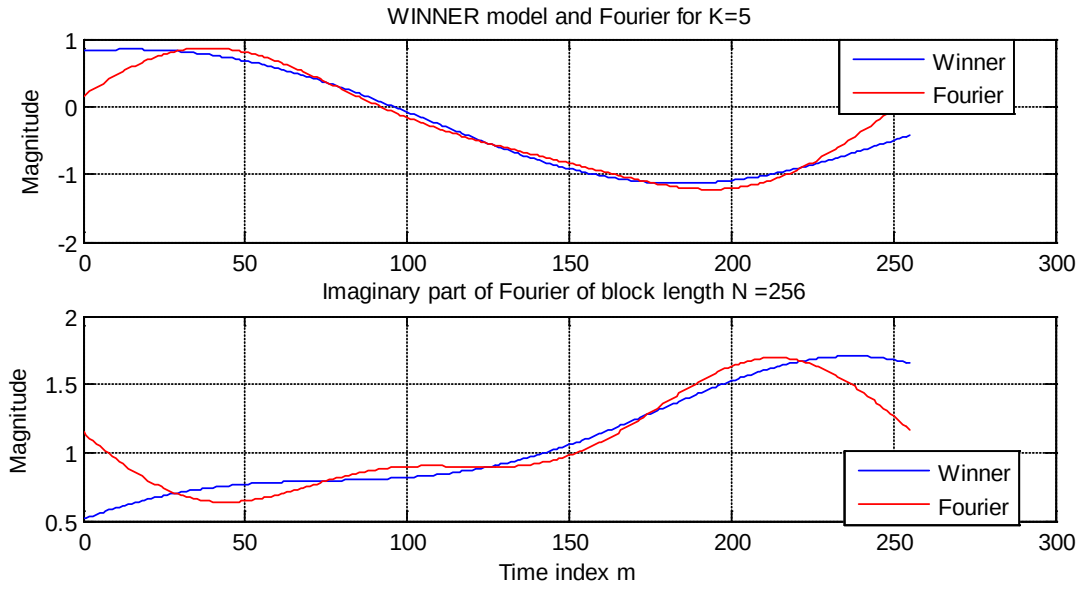


(e)

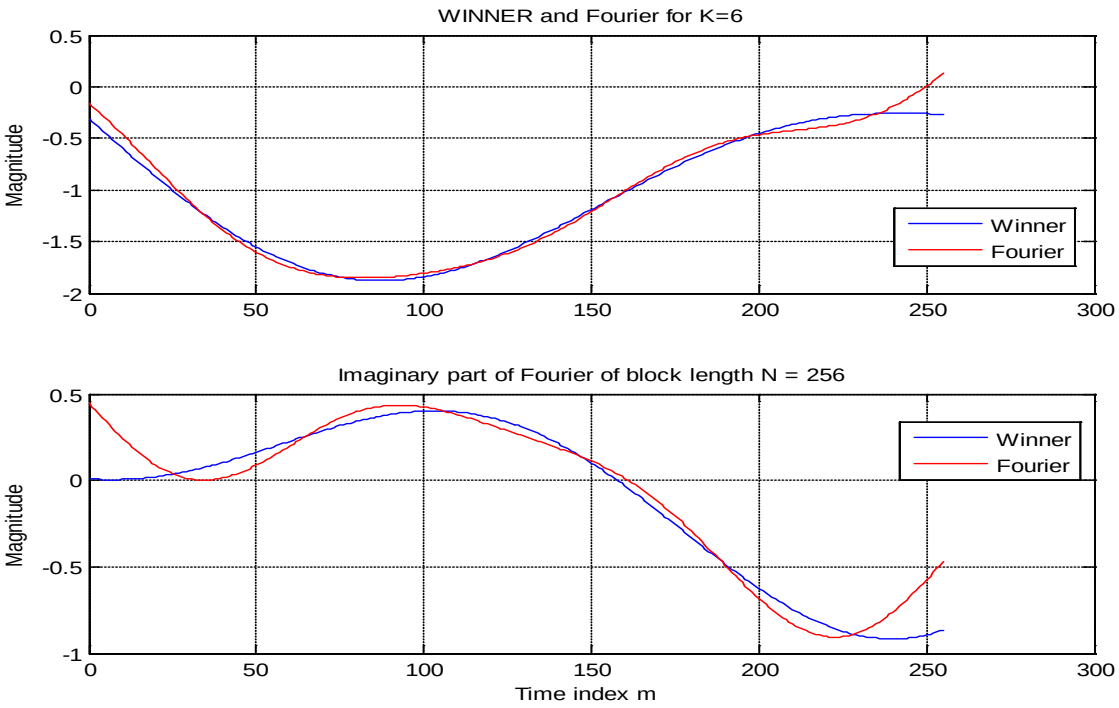


(f)

Figure 6.9 The fitting of WINNER model with Fourier basis expansion as function of time index *m*

a) For N = 256 and K = 1 b) For N = 256 and K = 2 c) For N = 256 and K = 3 d) N = 256 and K = 4 e) For N = 256 and K = 5 f) For N = 256 and K = 6.

This thesis also investigated the performance of the three channel estimation methods by comparison using the Mean Square Error (MSE) by using the Least-Squares method, so that we can get the result of the channel estimation performance by determining the channel estimation error values by averaging over 100 independent channel realizations according to:

$$MSE_N = \frac{1}{N}\sum_{m=0}^{N-1} E\left\{\left|h[m]-\tilde{h}[m]\right|^2\right\} \tag{6.2}$$

Where:

$$\begin{aligned} h[m] \qquad & m \in \{0,...,N-1\}, \text{ and } N = 256 \\ \tilde{h}[m] = \sum_{i=0}^{K-1} a_i u_i[n] \qquad & i \in \{0,....,K-1\}, \end{aligned} \tag{6.3}$$

To get the value of a coefficient $a_i$ which minimizes the channel estimate error, we have solved the equation:

$$E = \min \sum_{m=0}^{N-1}\left(h[m]-\sum_{k=0}^{K-1} a_i u_i[m]\right), \quad m \in \{o,....,N-1\}, \quad k \in \{0,.....,K-1\} \tag{6.4}$$

$$\frac{\partial E}{\partial a_i} = 2\sum_{m=0}^{N-1}\left(h[m]-\sum_{i=0}^{K-1} a_i u_i[m]\right)\left(-u_j[m]\right) = 0 \tag{6.5}$$

We may rewrite the Equation (6.5) as:

$$\sum_{m=0}^{N-1}\sum_{i=0}^{K-1} a_i u_i[m] u_j[m] = \sum_{m=0}^{N-1} h[m] u_j[m] \tag{6.6}$$

$$\sum_{i=0}^{K-1} a_i \sum_{m=0}^{N-1} u_i[m] u_j[m] = \sum_{m=0}^{N-1} h[m] u_j[m], \quad j \in \{0,....,K-1\} \tag{6.7}$$

We can represent Equation (6.7) into matrix form. We define the coefficient $a_i$ of the channel for all basis functions $K$ as:

$$\begin{pmatrix} \sum_{m=0}^{N-1} u_0^2(m) & \cdots & \sum_{m=0}^{N-1} u_0(m) u_{K-1}(m) \\ \vdots & \ddots & \vdots \\ \sum_{m=0}^{N-1} u_{K-1}(m) u_0 & \cdots & \sum_{m=0}^{N-1} u_{K-1}^2(m) \end{pmatrix} \begin{bmatrix} a_0 \\ \vdots \\ \vdots \\ a_{K-1} \end{bmatrix} = \begin{pmatrix} \sum_{m=0}^{N-1} h(m) u_0(m) \\ \vdots \\ \sum_{m=0}^{N-1} h(m) u_{K-1}(m) \end{pmatrix} \tag{6.8}$$

$$\begin{bmatrix} a_0 \\ \vdots \\ \vdots \\ \vdots \\ a_{K-1} \end{bmatrix} = \begin{pmatrix} \sum_{m=0}^{N-1} u_0^2(m) & \cdots & \sum_{m=0}^{N-1} u_0(m) u_{K-1}(m) \\ \vdots & \ddots & \vdots \\ \sum_{m=0}^{N-1} u_{K-1}(m) u_0 & \cdots & \sum_{m=0}^{N-1} u_{K-1}^2(m) \end{pmatrix}^{-1} \begin{pmatrix} \sum_{m=0}^{N-1} h(m) u_0(m) \\ \vdots \\ \sum_{m=0}^{N-1} h(m) u_{K-1}(m) \end{pmatrix} \tag{6.9}$$

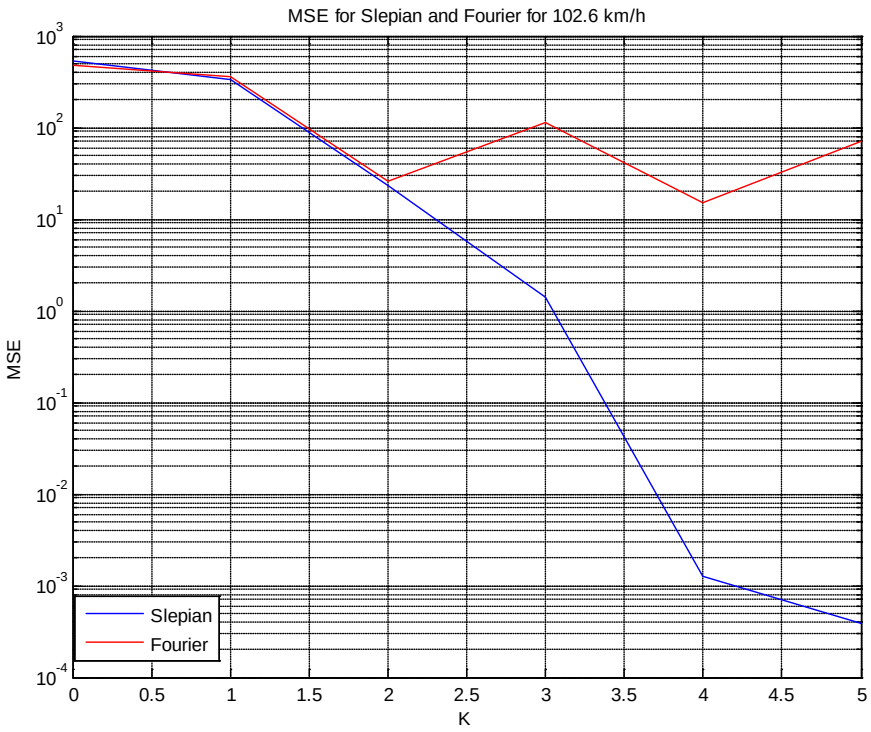


Figure 6.10 MSE as a function of basis functions K for Slepian and Fourier at 102.6 km/h

The following figures show the Mean Square Error (MSE) as a function for the various values of basis functions K with three different velocity of the user.

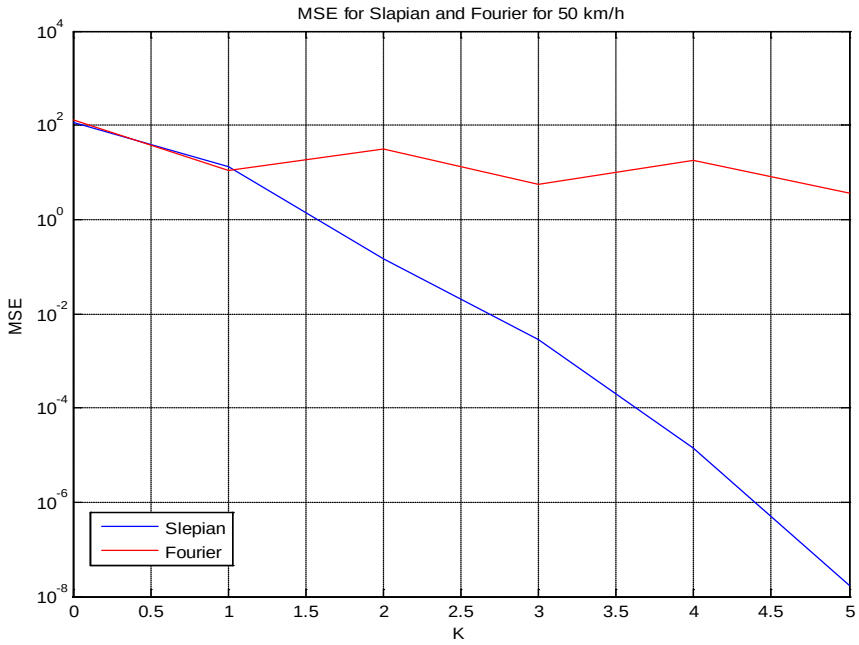


Figure 6.11 MSE as a function of basis functions K for Slepian and Fourier at 50 km/h

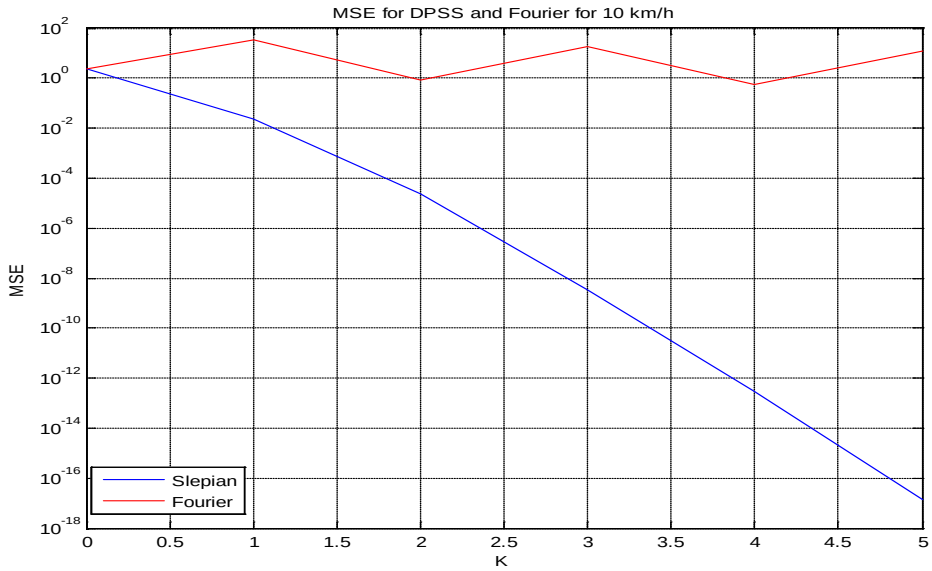


Figure 6.12 MSE as a function of basis functions K for Slepian and Fourier at 10 km/h

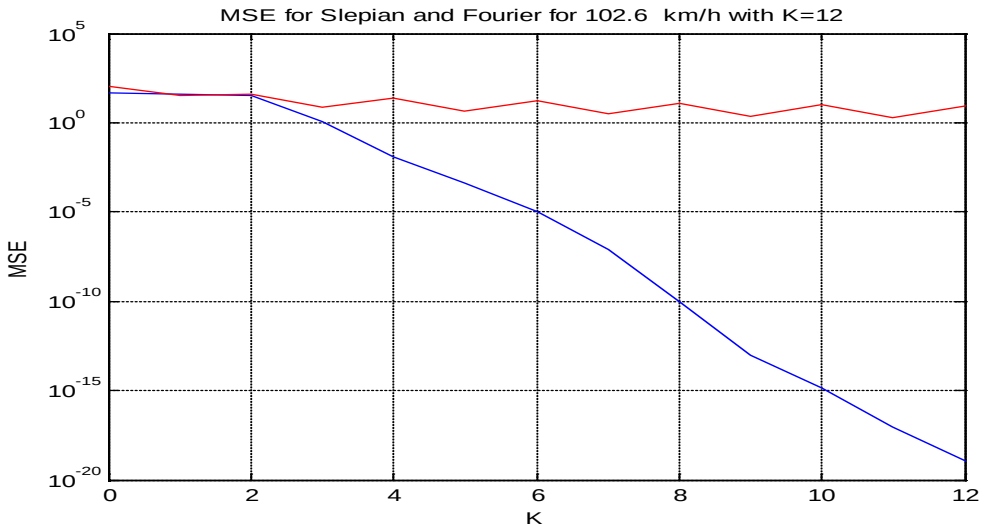


Figure 6.13 MSE as a function of K for Slepian and Fourier at 102.6 km/h with K = 12

The following tables show the values of the Mean Square Error as a function of basis function K at fixed velocity of 102.6 km/h.

| **K** | **1** | **2** | **3** | **4** | **5** |
|---|---|---|---|---|---|
| **Slepian** | 369.7556 | 135.8385 | 15.4088 | 0.67167 | 0.017933 |
| **Fourier** | 403.6928 | 142.1907 | 34.229 | 41.8081 | 19.0499 |

| **K** | **6** | **7** | **8** | **9** | **10** |
|---|---|---|---|---|---|
| **Slepian** | 0.0003408 | $4.38*10^{-4}$ | $4.41*10^{-8}$ | $3.10*10^{-10}$ | $2.21*10^{-12}$ |
| **Fourier** | 25.2482 | 13.6656 | 19.3345 | 10.0369 | 14.9512 |

| K | 11 | 12 | 13 | 14 | 15 |
|---|---|---|---|---|---|
| **Slepian** | $1.12*10^{-14}$ | $4.74*10^{-17}$ | $1.71*10^{-19}$ | $5.68*10^{-22}$ | 1.14*10 |
| **Fourier** | 8.7081 | 13.7921 | 6.9155 | 10.6407 | 6.263 |

Table 6 The values of MSE for both Slepian and Fourier at different values of basis functions

# 7 Discussion

The results from simulations can provide important data on three things, the Power spectrum of channel process of the WINNER model, the linear curve fitting, and the values of the Mean Square Error (MSE) using Least squares method.

## 7.1 Power spectrum of the channel process of the WINNER model

The Power spectrum of the channel process for the WINNER model fits exactly the value of the maximum normalized Doppler frequency $\nu_{D\max}$ of the Slepian basis expansion. During this study the maximum velocity of the user was investigated and it was found that the lower the velocity of the user, the less the $\nu_{D\max}$, and the slower the curve of the channel gain.

## 7.2 Fitting of the curves

From observing the curves we can see that with a small value of basis functions of K, the Slepian basis expansion is a suitable model for mobile wireless systems if compared to Fourier basic expansion. For the value of K = 4 the Slepian coincided with the curve of the WINNER model, while for K = 6 neither the real part nor the imaginary part of the Fourier basis expansion coincided with the curve of the WINNER model. In Figure 6.10 the curves for both the Slepian and Fourier are closed to each other up to K = 2, but after that the curves separate from each other. The simulations tell us that for low value of basis function K the Slepian had a better fit to the WINNER model than the Fourier did. Even for a large K value the Fourier does not fit a WINNER model curve.
From figure 6.10 we can see that, from K = 2 onwards the Fourier remains constant while the Slepian decreases towards to zero. The Slepian basic expansion if compared with the Fourier basis expansion is several magnitudes lower for all values of K. So the curves indicate that the maximum normalized one-sided Doppler bandwidth of Slepian basis expansion is a better model for modeling a mobile wireless communication system than the Fourier basis expansion.

## 7.3 The Mean Square Error (MSE)

The MSE in table 6 provides evidence that the Slepian basis expansion is better compared to the Fourier basis expansion because the MSE of Slepian is much less than that of Fourier. Part of the explanation can be found in [2, 22, Sec.5.4] concerning of the frequency leakage of the Fourier basis expansion, i.e. a truncated discrete Fourier transform (DFT). Table 6 also shows

the continual decrease of the MSE to the value of K. For The Fourier it is different, however, because the MSE does not decrease continually, especially for the even values of K. Even at 102.6 km/h when the value of K is increased to K = 12, the MSE curves for both Slepian and Fourier still did not coincide after K = 2.

# 8. Conclusion and Future work

## 8.1 Future work

In order to achieve a reliable communication system capable of meeting the demands of the future, it is important to estimate the time-variant channel as accurately as possible, i.e. as close to the true channel as possible. In order to estimate the channel accurately, the velocity of the user must be estimated. It is necessary to estimate the velocity of the user for the Slepian basis expansion because good performance of the Slepian depends on sequences of the Slepian basis expansion complying with the velocity of the user. For high data rates and high capacity of the system, many methods remain to be investigated. Future work to investigate the reduction in the length of Slepian sequences in a slow fading channel (i.e., in a lower mobility and when the Doppler frequency is small) is also important. Long Slepian sequences usually increase high decoding complexity [9]. This thesis has not compared the polynomial time-varying channel model with the WINNER model so that the future work should include even this model because the basis of polynomial is not restricted to time-limited and band-limited functions.

## 8.2 Conclusion

An important and crucial part of modern mobile wireless systems is channel estimation, which helps the system deliver high data rates and achieve the maximum transmission rate by accurately estimating the wireless channel. Slepian basis expansion and the WINNER model can be applied for Long Term evolution systems in the future. This investigation has been done by using three parameters, the maximum Doppler bandwidth $v_{D\max}$, velocity of the user $v_{\max}$,and the block length of $N$ = 256 symbols. The thesis evaluates and compares the performance of the three methods of channel estimation: Slepian basis expansion, Fourier basis expansion and the WINNER phase II model. It is concluded that Slepian basis expansion fits the WINNER model better than Fourier basis expansion at both a lower and higher values of K. The Fourier basis expansion does not fit well in either condition at both the beginning and at the end of the block length of sequences $N$ = 256 symbols.

The Slepian basis expansion fits particularly well at a lower mobility at 10 km/h than in a higher mobility at 102.6 km/h because the curve of the channel gain at 10 km/h is slower compare to 102.6 km/h. It is easier for detector or receiver to follow the channel at 10 km/h as shown in figure 6.6. At high mobility of 102.6 km/h, the value of maximum normalized one-sided Doppler bandwidth $v_{D\max}$ = 0.0039 for Slepian basis expansion and is exactly the same as the Power spectrum of the WINNER model, as shown in figure 6.3. The Slepian basis expansion fits especially well till basis functions K = 3 which is equivalent to the values of minimum signal space of the Slepian D´= 3. The curve in figure 6.10 behaves well compared to the theory of approximate dimension of minimum signal space D´. We have already seen that the higher the velocity of the user the larger the approximate dimension of the signal $D'$.

The performance comparison of the Slepian, Fourier basis expansion and WINNER model for the different number of the basis functions K were investigated. The investigation has used the Mean Square Error (MSE) with average over 100 independent channel realizations. As expected, the results from simulations are very interesting. The error between Slepian basis expansion and WINNER model was observed to be much smaller if compared to Fourier basis expansion for all three different velocities $v_{\max}$ of 102.6 km/h, 50 km/h and 10 km/h.

The MSE is just $3.41*10^{-4}$ for Slepian basis expansion compared to larger value of 25.2482 for Fourier for six basis functions (K = 6) at the velocity = 102.6 km/h. The MSE for Slepian becomes less for every value of basis functions K. For Fourier basis expansion it is quite different and varies considerably, especially with an even number of the basis functions. The Fourier basis expansion has poor performance because the energy from low- frequency Fourier coefficients leaks to the full frequency range [22, Sec 5.4]. The spectra leakage happens because of involvement of DFT and a leakage causes phase and amplitude errors at the beginning and at the end of data block [27].

# 9. References


[1] https//www.ist-winner.org/

[2] Thomas Zemen and Christoph F. Mecklenbräuker
Time-Variant Channel Estimation Using Discrete Prolate Spheroidal Sequences. IEEE Transactions on Signal Processing, Vol.53 no. 9, pp. 3597-3607, September 2005.

[3] David Tse and Pramod Viswanath
Fundamentals of Wireless Communication, Cambridge University Press, 2005. ISBN 13978-0-521-84527-4.

[4] Monson H. Hayes
Statistical Digital Signal Processing and Modeling, John Wiley & Sons, Inc. New York, NY, USA

[5] Borko Furht and Syed A. Ahson, Long Term Evolution: 3GPP LTE radio and cellular technology, published by Taylor & Francis Group, LLC 2009.

[6] Jens Zander, Ben Slimane and Lars Ahlin
Principle of wireless communications.

[7] Stefan Kaiser
Multi-Carrier CDMA Mobile Radio Systems-Analysis and Optimization of Detection, Decoding, and Channel Estimation. Munich Gemany, January 1998. Ph.D. thesis published with: VDI- Verlag, Dusseldorf. Germany. 1998. ISBN 3-18-353110-0.

[8] D. Kliazovich 1, F. Granelli, S. Redana and N. Riato, Cross-Layer Error Control Optimization in 3G LTE, IEE Global Telecommunication Conference, Trento 2007

[9] Jinho Kim, Chih-Wei, Wang and Wayne E. Stark.
Frequency Domain Channel Estimation for OFDM Based on Slepian Basis Expansion, University of Michigan, Ann Arbor.
Communication, 2007 ICC 107. IEEE ISBN: 1-4244-0353-7

[10] X. Ma, and G. Giannakis,
Maximum-diversity transmissions over doubly selective wireless channels, IEEE Trans. Inform. Theory, vol. 49 no. 7, pp.1832-1840, Jul.2003.

[11] Y. li, L. J.Climini Jr. and N. R. Sollengerger
Robust channel estimation for OFDM systems with rapid dispersive fading channels, IEEE Trans. Commun., vol. 46 no. 7, pp. 902-915, Jul. 1998.

[12] Thomas Zemen
OFDM Multi-User Communication Over Time-Variant Channel, PhD thesis, 2004. ISBN 3-902477-04-0

[13] J. Parsson
The mobile radio Propagation Channel, Pentech Press Publ., London, 1992

[14] W. Jakes
Microwave Mobile Communication, Wiley-Interscience, USA 1974

[15] Shinsuke Hara and Ramjee Prasad
Overview of Multicarrier CDMA, in IEEE Comm. Magazine, volume 35, no. 11, December 1997

[16] diracdelta.co.uk/science/source/r/e/rectangular%20window/source.html

[17] Spectral Analysis Statistical Signal Processing
http://www.mathworks.com/access/helpdesk/help/toolbox/signal/f12-6587.html

[18] John G. Proakis
Digital Communication, fourth edition, McGraw-Hill, New York USA 2001 ISBN 0-07-118183-0

[19] Theodore S. Rappaport

Wireless Communications, Principles and Practice, Prentice Hall, Upper Saddle River, NJ, USA 2002

[20] M. Alard and R. Lasalle
Principles of modulation and coding for digital broadcasting for mobile receivers, EBU Technical Review, number 224 pp.168-190. August 1987

[21] S.B Weinstein and P. M. Ebert
Data Transmission by Frequency-Division Multiplexing Using the Discrete Fourier Transform. IEEE Transactions on Communications, vol. COM-19. pp. 628-634, 1971.

[22] John G. Proakias and Dimitris G. Manolakis
Digital Signal Processing, Third edition, Englewood Cliffs, NJ: Prentice-Hall, 1996.

[23] D. Slepian
Prolate spheroidal wave functions, Fourier analysis, and uncertainty -V: The discrete case. Bell syst. Tech. J., vol.57 no.5 pp.1371-1430, May-Jun. 1978.

[24] Maréuane Debbah, Alcatel-Lucent Chair on Flexible Radio
Short introduction to OFDM
http://www.supelec.fr/d2ri/flexibleradio/cours/ofdmtutorial.pdf

[25] Yun Chiu, Dejan Markovich, Haiyun Tang, Ning Zang
EE225C Final Project Report, 12 December 2000
Retrieved from
http://bwrc.eecs.berkeley.edu/classes/ee225c/Lectures/Lec16_ofdm.pdf

[26] B.G. Molnár, I. Frigyes, Z. Bodnár, Z. Herczku
The WSSUS channel model: comments and a general, Budapest Hungary

[27] M. Niedzwiecki
Identification of Time-varying Processing, New York, Wiley 2000.

[28] J.Salo,G.Del Galdo, J.Salmi, P. Kyösti, Marko Milojevic. Daniela Laselva and Christian Shnejder
Matlab implementation of 3GPP Spatial channel Model
(3GPP TR 25.996). On-line, January hpp://www.tkk.fi/Units/Radio/scm/.

[29] Overview of 3GPP Release 8 V0.0.3, November 2008

[30] John G. Proakis and Masoud Salehi
Communication Systems Engineering, second edition, Prentice Hall, 2002.

[31] http://en.wikipedia.org/wiki/3GPP_Long_Term_Evolution

[32] http://en.wikipedia.org/wiki/4G

[33] Tan, M; and Bar-Ness, Y.
Optimal power distribution control under different total power constraints strategies for multicode MC-CDMA, Wireless Com. And net. Conference, 2004. WCNC. 2004 IEEE, vol. 3,no., pp. 1376-1381Vol 3.

[34] http://en.wikipedia.org/wiki/Multi-carrier_code_division_multiple_access

[35] Markku Pukkila
Channel estimation Modeling, Nokia research center HUT 19.12.2000.

[36] W. C. Jakes (2nd) and D. Cox
Microwave Mobile Communications. Wiley-IEEE Press, New York 1994

[37] Hyung G. Myung
Technical Overview of 3GPP Long Term Evolution (LTE), Feb. 8, 2007.

[38] Israel Koffman and Vincentzio Roman
Broadband Wireless Access Solutions Based on OFDM Access in IEEE 802.16, IEEE Commun. Mag., vol. 40, no. 4, April. 2002, pp. 96-103

[39] P. A. Bello

Characterization of randomly time-variant linear channels, IEEE Trans. on Commun., vol.11, no. 4, pp. 360-393, Dec. 1963
[40] A. Thomson
Spectrum estimation and harmonic analysis, Proc. IEEE, vol. 70, pp. 1055-1096, 1982
[41] Yushi Shen and Ed Martinez
Channel Estimation in OFDM Systems, Rev. 0, 1/2006

# 10 APPENDIX

A.1 The developers of the WINNER I within WINNER I work package 5 (WP5) are the Royal Institute of technology (KTH), Elektrobit, Helsinki University of technology, Nokia, Swiss Federal Institute of Technology (ETH), and Technical University of Ilmenau.
For the WINNER II, five partners were involved for extending the WINNER I model features, frequency range from 2 to 6 GHz , and the number of scenarios are Elektrobit, University of Oulu / Centre for Wireless Communications (CWC), Technical University of Iimenau, Nokia, and Communication Reacherch Centre (CRC) Canada.

B.1 Propagation scenario
A1 In the building (Indoor small offices and residence)
A2 Indoor to outdoor
B1 Hotspot (Typical urban micro-cell)
B2 Bad urban micro-cell
B3 Indoor hotspot (Large indoor hall)
B4 Out door to indoor (-Outdoor typical urban, -Indoor A1)
B5a Stationary Feeder (LOS stat., feeder, rooftop to rooftop)
B5b Hotspot, Metropol (LOS stationary feeder, street-level to street-level)
B5C Hotspot, Metropol (LOS stationary Feeder, below rooftop to street-level)
B6d Hotspot, Metropol (NLOS stationary Feeder, above rooftop to street-level)
B5f Feeder link BS -> FRS. Approximately RT to RT level
C1 Suburban macro-cell
C2 Typical urban macro-cell
C3 Bad urban macro cell
C4 Urban macro outdoor to indoor
D1 Rural macro-cell)
D2 a) Moving networks (BS - MRS, rural)
b) Moving networks (MRS - BS, rural)

C2-Urban macro-cell
The CDL parameters of the LOS and NLOS conditions are given below:

| Cluster # | Delay [ns] | | | Power [dB] | | | AoD [°] | AoA [°] | Ray power [dB] | | Cluster ASD = 6° | Cluster ASA = 12° | XPR = 8 dB |
|---|---|---|---|---|---|---|---|---|---|---|---|---|---|
| 1 | 0 | | | 0.0 | | | 0 | 0 | -0.08* | -30.6** | | | |
| 2 | 0 | 5 | 10 | -16.2 | -18.4 | -20.2 | -24 | -120 | | -26.2 | | | |
| 3 | 30 | | | -15.3 | | | 26 | 129 | | -28.3 | | | |
| 4 | 85 | | | -16.7 | | | -27 | -135 | | -29.7 | | | |
| 5 | 145 | 150 | 155 | -18.2 | -20.4 | -22.2 | 26 | -129 | | -28.2 | | | |
| 6 | 150 | | | -18.2 | | | 28 | 141 | | -31.2 | | | |
| 7 | 160 | | | -15.3 | | | 26 | -129 | | -28.3 | | | |
| 8 | 220 | | | -23.1 | | | -32 | -158 | | -36.1 | | | |

* Power of dominant ray

** Power of each other ray

Table C.2.1 Scenario C2: LOS Clustered delay line model

| Cluster # | Delay [ns] | | | Power [dB] | | | AoD [°] | AoA [°] | Ray power [dB] | Cluster ASD = 2° | Cluster ASA = 15° | XPR = 7 dB |
|---|---|---|---|---|---|---|---|---|---|---|---|---|
| 1 | 0 | | | -6.4 | | | 11 | 61 | -19.5 | | | |
| 2 | 60 | | | -3.4 | | | -8 | 44 | -16.4 | | | |
| 3 | 75 | | | -2.0 | | | -6 | -34 | -15.0 | | | |
| 4 | 145 | 150 | 155 | -3.0 | -5.2 | -7.0 | 0 | 0 | -13.0 | | | |
| 5 | 150 | | | -1.9 | | | 6 | 33 | -14.9 | | | |
| 6 | 190 | | | -3.4 | | | 8 | -44 | -16.4 | | | |
| 7 | 220 | 225 | 230 | -3.4 | -5.6 | -7.4 | -12 | -67 | -13.4 | | | |
| 8 | 335 | | | -4.6 | | | -9 | 52 | -17.7 | | | |
| 9 | 370 | | | -7.8 | | | -12 | -67 | -20.8 | | | |
| 10 | 430 | | | -7.8 | | | -12 | -67 | -20.8 | | | |
| 11 | 510 | | | -9.3 | | | 13 | -73 | -22.3 | | | |
| 12 | 685 | | | -12.0 | | | 15 | -83 | -25.0 | | | |
| 13 | 725 | | | -8.5 | | | -12 | -70 | -21.5 | | | |
| 14 | 735 | | | -13.2 | | | -15 | 87 | -26.2 | | | |
| 15 | 800 | | | -11.2 | | | -14 | 80 | -24.2 | | | |
| 16 | 960 | | | -20.8 | | | 19 | 109 | -33.8 | | | |
| 17 | 1020 | | | -14.5 | | | -16 | 91 | -27.5 | | | |
| 18 | 1100 | | | -11.7 | | | 15 | -82 | -24.7 | | | |
| 19 | 1210 | | | -17.2 | | | 18 | 99 | -30.2 | | | |
| 20 | 1845 | | | -16.7 | | | 17 | 98 | -29.7 | | | |

Table C.2.2 Scenario C2: NLOS Clustered delay line model

| Scenario | | DS (ns) | AS at BS (°) | AS at MS (°) | ES at BS (°) | ES at MS (°) |
|---|---|---|---|---|---|---|
| A1 | LOS | 40 | 44 | 45 | 8 | 9 |
| | NLOS | 25 | 53 | 49 | 11 | 13 |
| A2/B4[#]/C4 | NLOS | 49/240[∇] | 58 | 18 | 10 | 10 |
| B1 | LOS | 36 | 3 | 25 | | |
| | NLOS | 76 | 15 | 35 | | |
| B3 | LOS | 27 | 17 | 38 | 21.2 | |
| | NLOS | 39 | 12 | 50 | 22.3 | |
| C1 | LOS | 59 | 6 | 30 | | |
| | NLOS | 75 | 8 | 45 | | |
| C2 | LOS | 41 | 10 | 50 | | |
| | NLOS | 234 | 8 | 53 | | |
| D1 | LOS | 16 | 6 | 16 | | |
| | NLOS | 37 | 9 | 33 | | |
| D2 | LOS | 39 | 5 | 32 | | |

[#]AS at BS denotes indoor azimuth spread and As at MS denotes outdoor azimuth spread

[∇] In case column A2/B4/C4 contains two parameter values, the left value corresponds to A2/B4 microcell and the right value to C4 macrocell.

Table C.2.3 Medium output value of large-scale parameters

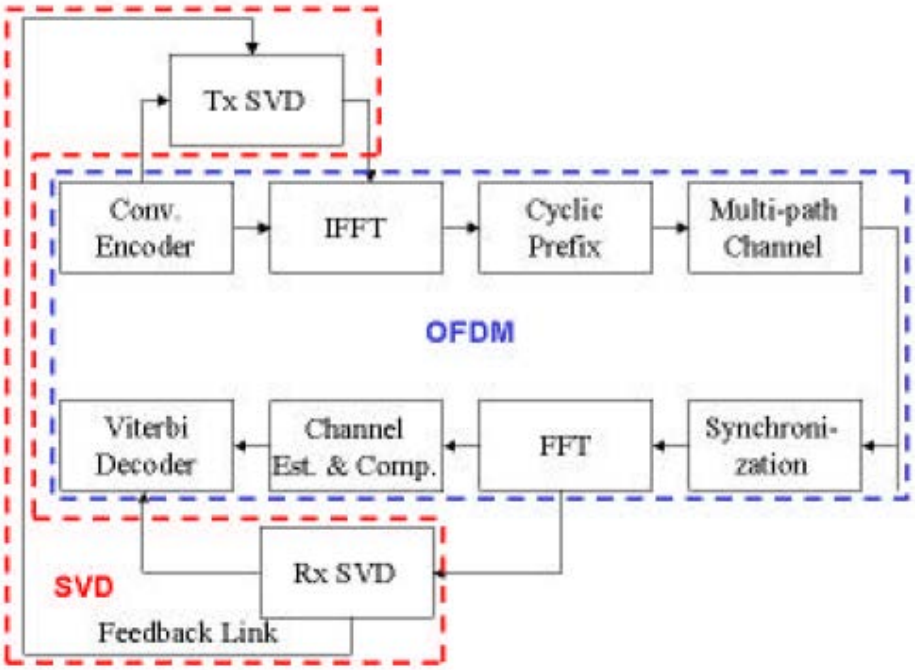


Figure C.1 Block diagram of the OFDM System [40]

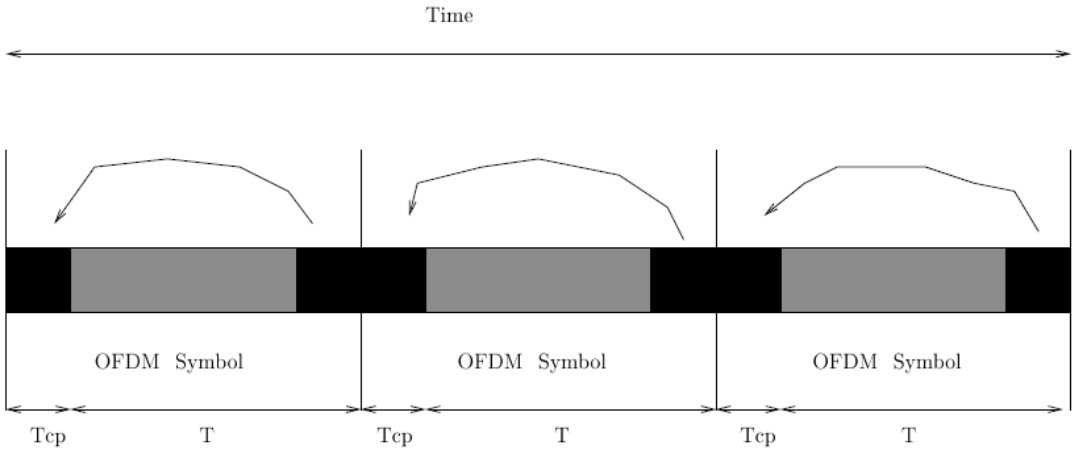


Figure C.2 Time representation of OFDM [39]

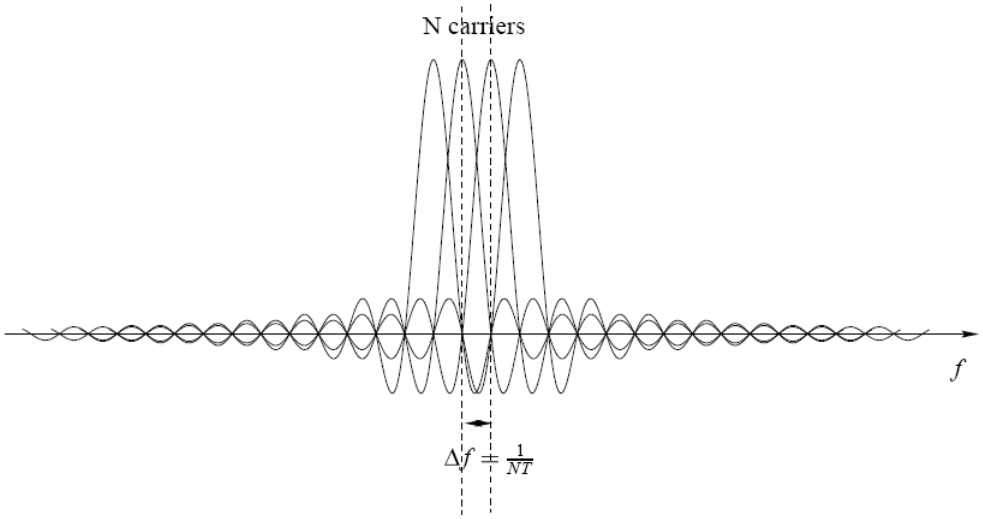


Figure C.3 Frequency representation of OFDM [39]